Published in final edited form as:
Annu Rev Physiol. 2015 February 10; 77: 29–55. doi:10.1146/annurev-physiol-021014-071622.

Mechanisms of Ventricular Arrhythmias: From Molecular Fluctuations to Electrical Turbulence

Zhilin Qu[1] and **James N. Weiss**[1,2]

Zhilin Qu: zqu@mednet.ucla.edu

[1]Department of Medicine (Cardiology), David Geffen School of Medicine, University of California, Los Angeles, California 90095

[2]Department of Physiology, David Geffen School of Medicine, University of California, Los Angeles, California 90095

Abstract

Ventricular arrhythmias have complex causes and mechanisms. Despite extensive investigation involving many clinical, experimental, and computational studies, effective biological therapeutics are still very limited. In this article, we review our current understanding of the mechanisms of ventricular arrhythmias by summarizing the state of knowledge spanning from the molecular scale to electrical wave behavior at the tissue and organ scales and how the complex nonlinear interactions integrate into the dynamics of arrhythmias in the heart. We discuss the challenges that we face in synthesizing these dynamics to develop safe and effective novel therapeutic approaches.

Keywords

ventricular arrhythmias; sudden cardiac death; multiscale dynamics; nonlinear dynamics; chaos

1. INTRODUCTION

Cardiac arrhythmias have been recognized as a key complication of heart diseases for centuries (1, 2). Generally defined, cardiac arrhythmias refer to conditions in which the electrical activity of the heart becomes too slow, too fast, and/or too irregular. Slow heart rhythms can be readily treated with electronic pacemakers, but rapid heart rhythms that culminate in atrial fibrillation or ventricular fibrillation (VF), in which the electrical activity in the atria or ventricles becomes turbulent, remain leading causes of morbidity and mortality, including sudden cardiac death, particularly in industrialized countries (3). From the first demonstration of electrical activity of the heart in 1856 (1) to today's modern technologies unraveling the genetic basis of many cardiac arrhythmias (4, 5), this problem has been a major focus of medicine for more than a century. However, successful

DISCLOSURE STATEMENT

The authors are not aware of any affiliations, memberships, funding, or financial holdings that might be perceived as affecting the objectivity of this review.

pharmacological treatment is still problematic. Current antiarrhythmic drugs have limited effectiveness, and many can have unintended proarrhythmic effects (6, 7). The most effective treatment for VF is an implantable cardioverter defibrillator (ICD), which can promptly and effectively terminate life-threatening arrhythmias. However, 80% of patients who will die suddenly each year in the United States do not meet current clinical criteria for prophylactic implantation of an ICD (8); moreover, even among those who do meet such criteria, only one in five ICDs will deliver a life-saving shock because of the difficulty in identifying those at highest risk (9). Additionally, ICD treatment is expensive and has significant morbidity.

The limited effectiveness of biologically based antiarrhythmic therapies, as opposed to bioengineering-based strategies, is related to the ubiquitous problem in biomedicine that the relevant biological targets for drug or gene therapy exist at the molecular scale, whereas the arrhythmias exist at the organ scale. Predicting how the behavior of a molecule will affect the properties of the organ is very complex because at each more integrated level, from molecule to molecular signaling complex to organelle to cell to tissue to organ to organism, qualitatively new properties emerge from the complex nonlinear interactions between properties at that level of integration and properties at the next-higher level of integration. In other words, the heart, as is any other organ in the body, is regulated at multiple spatial and temporal scales, and each scale has its own dynamics that then give rise to the dynamics at the next scale.

In this review article, we summarize our current understanding of ventricular arrhythmias, focusing on the multiscale and complex dynamic nature of the problem. After a brief summary of the multiscale dynamics in the heart, we then deconstruct the excitation dynamics in the reverse order: tissue-scale electrical wave dynamics, cellular-scale action potential dynamics, and subcellular- and molecular-scale dynamics. The goal is to illustrate, in a stepwise fashion, how the higher-scale dynamics emerge from lower-scale dynamics. We discuss the challenges and the potential for nonlinear dynamics, combined with new systems approaches, to lead to the development of robust and effective therapeutics. The article involves some important concepts of nonlinear dynamics relevant to arrhythmias (10), such as dynamic instabilities, bifurcation, chaos, synchronization, criticality, and basins of attraction. To help the readers who are not familiar with these concepts, they are explained in more detail in the Supplemental Text (follow the Supplemental Material link from the Annual Reviews home page at http://www.annualreviews.org).

2. MULTISCALE DYNAMICS IN THE HEART

The dynamics of excitation and contraction at different scales in the heart have distinct features. At the molecular scale, dynamics is governed mainly by thermodynamic fluctuations. For instance, ion channels open and close randomly (Figure 1*a*), and thousands of ion channels and ion transporters are distributed in the cell membrane to generate ionic currents for the action potential (Figure 1*b*). The channels and transporters are typically organized into molecular signaling complexes regulating their activity. In addition to the surface plasma membrane, these molecular signaling complexes often form clusters in intracellular organelles, such as the sarcoplasmic reticulum (SR) and mitochondria. These

ion channel clusters open and close collectively to result in organelle-scale dynamics, such as calcium (Ca^{2+}) sparks and mitochondrial flickers (11). For example, a Ca^{2+} spark (Figure 1*c*) is a Ca^{2+} release event of a Ca^{2+} release unit due to the collective opening of the ryanodine receptors (RyRs) triggered by the opening of the associated L-type Ca^{2+} channel cluster or by high intracellular Ca^{2+}. Under normal conditions, the L-type Ca^{2+} channel–triggered Ca^{2+} sparks integrate to give rise to the whole-cell Ca^{2+} transient (Figure 1*b*). Under diseased conditions and/or high intracellular Ca^{2+} load, the Ca^{2+} sparks organize to form different types of intracellular Ca^{2+} waves (Figure 1*d*) to generate whole-cell Ca^{2+} oscillations [the analogy for mitochondria is mitochondrial depolarization waves and oscillations (12)].

At the cellular scale, the subcellular dynamics couple with surface membrane ionic currents to result in various excitation and contraction dynamics. Under normal conditions, a ventricular myocyte is excitable: A normal action potential and a corresponding Ca^{2+} transient triggering contraction are generated in response to a stimulus (Figure 1*b*). The action potential morphology and duration are heterogeneous throughout the heart, with epicardial but not endocardial myocytes tending to exhibit a spike-and-dome morphology (right panel in Figure 1*b*). Under certain diseased conditions when outward currents are reduced and/or inward currents are increased, voltage depolarizations (oscillations) can occur during the repolarization phase of the action potential, termed early afterdepolarizations (EADs) (Figure 1*e*). During the diastolic phase, a spontaneous Ca^{2+} wave elevates intracellular Ca^{2+}, which increases the Na^{+}-Ca^{2+} exchange current (I_{NCX}) to cause a voltage depolarization termed a delayed afterdepolarization (DAD) (Figure 1*e*). If the Ca^{2+} transient is large enough to depolarize the voltage to the threshold for Na^{+} channel activation, a full action potential occurs, which is termed triggered activity. An EAD, if its takeoff potential is low and amplitude is large, can also cause triggered activity. During rapid pacing, the action potential duration (APD) of a normal ventricular myocyte may exhibit a long-short-long-short pattern termed APD alternans (Figure 1*f*). Under diseased conditions, APD alternans can often occur at much slower heart rates. A ventricular cell can also become oscillatory (Figure 1*g*) due to aberrant ionic current or Ca^{2+} cycling properties, termed automaticity.

At the tissue and organ scales, the cellular dynamics combine with tissue heterogeneities and cell coupling properties to generate the electrical wave dynamics underlying normal sinus rhythm, as well as different types of arrhythmias. During normal sinus rhythm, the impulses originating from the sinoatrial node follow an anatomically defined conduction pathway culminating in synchronous excitation of the ventricles. These excitation waves are termed rectilinear (or planar) waves (Figure 2*a*). Under diseased conditions, different types of electrical waves can occur in the ventricles, resulting in different types of ventricular arrhythmias. The first type of wave is termed a target wave (or focal excitation), in which spontaneous excitation originates from a local region of the ventricles due to heterogeneities in cellular properties and propagates outward to excite other regions of the heart (Figure 2*b*). The second type of wave is an excitation wave propagating around an obstacle, termed anatomical reentry (Figure 2*c*). The third type of wave does not require heterogeneities or an obstacle and can even occur in completely homogeneous tissue; this type is termed a spiral

wave (Figure 2*d*) or sometimes a rotor or functional reentry. Because the heart is a three-dimensional object, the spiral wave in two-dimensional tissue is technically a scroll wave in the real heart (Figure 2*e,f*), but here we use spiral wave to refer to both.

The dynamics at a higher scale depend on the dynamics at lower scales, but the information flow is bidirectional so that the dynamics at a lower scale are also modulated by the dynamics at the higher scales. For example, EADs in an action potential are caused by aberrant ion currents and Ca^{2+} cycling properties, but the occurrence of EADs can bring more Ca^{2+} into the cell to potentiate Ca^{2+} waves due to L-type Ca^{2+} channel opening during the EADs. Furthermore, besides the typical Ca^{2+} cycling, action potential, and electrical wave dynamics shown in Figures 1 and 2, more complex dynamics can emerge due to heterogeneities and dynamic instabilities. These dynamics at different scales play critical roles in initiating arrhythmias, as well as giving rise to different types of arrhythmias. Therefore, to understand the mechanisms of arrhythmias and to develop molecularly based therapeutics, one needs to understand how molecular behaviors relate to electrical wave dynamics; i.e., one needs to relate the dynamics at each lower scale (in both time and space) to the dynamics at the next higher scale, sequentially from molecule to organism. For example, to understand how a mutation in RyRs is linked to arrhythmias, one needs to understand, in sequence, the following: how the mutation modifies the opening and closing properties of RyRs; how RyRs in a cluster interact with each other to affect Ca^{2+} spark behavior both normally and when various signaling pathways are activated; how Ca^{2+} sparks organize into Ca^{2+} waves and oscillations; how Ca^{2+} waves and oscillations affect the cellular action potential dynamics, such as alternans, EADs, and DADs; and finally how these cellular action potential dynamics synchronize at the tissue and organ levels to generate the electrical wave dynamics leading to different types of arrhythmias. In the sections below, we summarize our current understanding of the multiscale dynamics in the heart to illuminate first how the dynamics at a higher scale emerge from the dynamics of a lower scale and then how the dynamics at the higher scale feed back to modulate the properties at the lower scale.

3. ARRHYTHMOGENIC ELECTRICAL WAVE DYNAMICS AT THE TISSUE AND ORGAN SCALES

Different electrical wave dynamics at the tissue and organ scales give rise to different types of arrhythmias. These wave dynamics are caused by either preexisting tissue heterogeneities or dynamic instabilities or their interactions, which are summarized in the sections below.

3.1. Focal Excitations Due to Triggered Activity and Automaticity

A focal excitation (Figure 2*b*) is a spontaneous firing of a group of cells in cardiac tissue. Spontaneous firing can be due to either triggered activity or automaticity. Under normal conditions, thousands of cells need to fire synchronously to overcome the strong sink effect of the adjacent unexcited cells, but under conditions of weak gap junction coupling, such as in fibrotic or ischemic tissue, the number of the spontaneously firing cells required to form a focal excitation is substantially reduced (13).

Traditionally, focal excitations have been thought to require heterogeneous tissue, i.e., one region of the tissue exhibiting spontaneous firing that propagates into surrounding quiescent regions. Intuitively, if all cells are identical and therefore spontaneously fire simultaneously in a homogeneous tissue, the whole tissue fires together, and no localized focus can form. However, focal excitations can also occur in homogeneous tissue via self-organizing pattern formation (Supplemental Figure 1*a*). Our recent study (14) showed that when the action potential develops EADs, the dynamics at the cellular level can be chaotic such that at the tissue level, regional chaos synchronization results in the formation of islands of long APD with EADs next to regions with normal APD without EADs, forming a complex spatiotemporal pattern. The EADs propagate out of the islands, forming a pattern of multiple, shifting focal excitations. The foci formed via this mechanism are not stable but vary dynamically in space and time due to the spatiotemporal chaotic dynamics. In contrast, focal excitations purely due to a tissue heterogeneity remain fixed in space. This dynamic feature agrees with the experimental observations of focal arrhythmias in drug-induced long-QT (LQT) syndrome, in which multiple foci arising dynamically from different locations occur in space and time (15, 16). Tissue heterogeneities and random ion channel fluctuations potentiate these dynamics (17, 18). The dynamic mechanisms of multiple foci nicely account for two features of polymorphic ventricular tachycardia (VT): (*a*) the observation that polymorphic VT can be sustained for long periods in tissue, even though single cells usually exhibit only one or several EAD-triggered action potentials (17), and (*b*) the frequent spontaneous termination of polymorphic VT, in particular torsade de pointes (19).

A clear example of heterogeneity interacting with dynamics is bidirectional VT in catecholaminergic polymorphic VT (CPVT), in which two focal excitations can perpetuate each other to form a stable reciprocal firing pattern (20). A simulation study by Baher et al. (21) demonstrated this mechanism. Specifically, as the heart rate increases, a focal excitation due to a DAD occurs at a certain location (e.g., the left bundle branch), which propagates reciprocally to the contralateral (right) bundle branch and causes a focal excitation there via the same mechanism. The excitation from the right then propagates to the left and causes another focal excitation in the left branch, and so on in a reciprocating ping-pong fashion.

3.2. Reentry

Two general categories of reentry occur in cardiac tissue: reentry around an obstacle (anatomical reentry; Figure 2*c*), such as reentry using a specialized pathway (e.g., a bypass tract or around a scar), and spiral wave reentry (also known as scroll wave, rotor, or functional reentry; Figure 2*d*). Anatomical reentry was first demonstrated experimentally in an annulus of cardiac tissue by Mines (22) approximately a century ago. In many cases, anatomical reentry is stable, resulting in monomorphic VT. However, depending on the path length of the reentry circuit relative to the wavelength of the impulse, reentry may become unstable, leading to more complex morphologies of arrhythmias, such as polymorphic VT and VF.

Spiral waves are a generic feature of wave dynamics in excitable media that can occur in both homogeneous tissue and heterogeneous tissue. Spiral waves were first demonstrated in chemical reactions (23) and later in cardiac tissue (24). Spiral waves can be stable, resulting

in a periodic behavior manifesting as monomorphic VT, but can also be unstable. In the latter case, the spiral wave meanders and drifts and can spontaneously break up into multiple spiral waves—a turbulent state of electrical waves. A meandering or drifting spiral wave can give rise to polymorphic VT or torsade de pointes, whereas frank breakup along the arm of a spiral wave results in fibrillation due to the generation of new spiral waves and/or fibrillatory conduction block.

Computer modeling as well as experimental studies have shown that the slope of the APD restitution curve is a key parameter that determines the stability of the spiral wave reentry in cardiac tissue such that a spiral wave becomes more unstable as the slope of APD restitution curve becomes steeper (25, 26). APD restitution is defined as the relationship between the APD and its preceding diastolic interval (see Supplemental Figure 2 for more detailed definition), which is a measure of the state of ion channel recovery from their openings in the previous action potential. When the APD restitution curve is steep enough, there is spiral wave breakup (Supplemental Figure 1*b*,*d*,*e*), in which a turbulent electrical state maintained by irregular spiral waves (or wavelets) appears and disappears in a chaotic manner. Spiral breakup as a mechanism of fibrillation agrees with Moe et al.'s (27) original multiple wavelets hypothesis, in which fibrillation is characterized by multiple wandering wavelets in the heart. However, tissue heterogeneities can also promote spiral wave meandering and wave breaks. For example, in a tissue with large refractory gradient, fibrillatory conduction block can occur. In this scenario, a fast spiral wave generates higher-frequency excitations that are unable to propagate 1:1 into surrounding regions with longer refractory periods, resulting in wave breaks generating turbulent wave patterns (Supplemental Figure 1*c*). This mechanism is termed mother-rotor fibrillation (2). Because cardiac tissue is heterogeneous, the dominant mechanism depends on the specific disease conditions, and in some conditions, both mechanisms may work in synergy to generate the electrical turbulence of VF.

3.3. Biexcitability

Biexcitability is a novel wave conduction behavior demonstrated in recent studies (28–30). In both atrial and ventricular tissue, normal wave conduction is driven mainly by the Na^+ current (I_{Na}), which mediates the initial rapid upstroke of the action potential. Under certain conditions—such as LQT syndrome, in which prolonged APD and EADs occur due to reduced repolarization reserve—cells can develop two stable resting membrane potentials: one typically at approximately −80 mV and one at approximately −50 mV (31). Under these conditions, bistable wave propagation can occur; i.e., a slow conduction mediated by L-type Ca^{2+} current ($I_{Ca,L}$) from the more depolarized resting potential (at which I_{Na} is mostly inactivated) and a fast conduction mediated by both I_{Na} and $I_{Ca,L}$ from the fully repolarized resting potential occur in the same tissue. This behavior is therefore referred to as biexcitability. Chang et al. (28) demonstrated this behavior by showing, in computer simulations, that in a homogeneous tissue two distinct types of spiral waves can be induced, depending on the method of initiation. In the first type of fast spiral wave (Supplemental Figure 3*a*), voltage recovers close to the resting potential (−80 mV), and both I_{Na} and $I_{Ca,L}$ are activated. In the second type of slow spiral wave (Supplemental Figure 3*b*), however, voltage recovers only to approximately −50 mV. Because I_{Na} is inactivated above −60 mV,

only $I_{Ca,L}$ is activated, which results in a slower propagation. Under some conditions, both types of conduction occur interchangeably in the same tissue (Supplemental Figure 3*c*). This behavior was experimentally observed in cultured myocyte monolayers (28, 29) and can be seen in recordings during arrhythmias in LQT syndrome (16, 32). Biexcitability may provide a mechanism for torsade de pointes and may explain why torsade de pointes often spontaneously terminates but sometimes degenerates into VF (28, 29).

3.4. Arrhythmia Initiation: Trigger and Substrate Interactions

Although understanding reentrant and focal electrical wave behaviors during arrhythmias is important, even more important is understanding how these waves and foci are initiated because from the therapeutic viewpoint, the ideal strategy is to prevent the initiation of arrhythmias. Generally speaking, initiation of reentry requires two factors: a critically timed trigger such as a premature ventricular complex (PVC) and a tissue substrate exhibiting dispersion of refractoriness. On the basis of past studies, we can summarize the most relevant settings as follows.

3.4.1. Induction of arrhythmias around an anatomical obstacle—Reentry around an obstacle can form by different mechanisms (Figure 3*a*). When the tissue around the obstacle is homogeneous and the pathways are wide, a PVC can successfully conduct through both pathways (case *i* in Figure 3*a*) and does not induce reentry. When the tissue around the obstacle is electrically heterogeneous, however, unidirectional conduction block of a properly timed PVC can occur due to dispersion of refractoriness, allowing the antegrade impulse to conduct retrogradely into the blocked pathway, initiating reentry (case *ii* in Figure 3*a*) (22). Another scenario is source-sink mismatch (33, 34), in which one of the pathways has a very narrow exit (case *iii* in Figure 3*a*) and the impulse fails to propagate out of the narrow pathway due to the strong sink effect from the cells outside the exit (i.e., a small number of cells at the exit of the narrow pathway provides the electrical source for a large number of cells outside, and thus the source is weaker than the sink). However, the impulse from the other pathway can enter into the narrow pathway because the source from the outside cells is strong enough (i.e., a large number of cells outside provides the electrical source for a small number of cells in the narrow pathway, and thus the source is stronger than the sink). Because of this source-sink mismatch, reentry can form. This mechanism of reentry initiation can underlie concealed Wolff-Parkinson-White syndrome, a common cause of paroxysmal supraventricular tachycardia, as well as reentry in scarred and fibrotic tissue, such as in the border zone of an infarct.

3.4.2. Induction of arrhythmias by a trigger in heterogeneous tissue without anatomic obstacles—In tissue with no obstacles or specialized pathways, unidirectional conduction block can still occur due to dispersion of refractoriness (35). A typical scenario is shown in Figure 3*b*: The central region of the tissue has a longer refractory period so that a PVC originating from a peripheral location may fail to propagate through the central region and propagate around it, reentering from the other side to form so-called figure-of-eight reentry. For reentry to form by this mechanism, the central region needs to be large enough and the PVC timed in a proper window termed the vulnerable window.

3.4.3. Induction of arrhythmias by a trigger and substrate arising from the same process—In the above two mechanisms, the trigger and the substrate emanate from two separate etiologies. In a third mechanism of reentry initiation, both the trigger and the substrate arise from the same cause. For example (Figure 3*c*), if the cells in the central region of a tissue exhibit EADs, but asymmetrical heterogeneities in the tissue alter electrical loading conditions (source-sink mismatch), EADs can propagate outward from one side of the heterogeneous region, but not from the other, leading to initiation of reentry. This scenario has been demonstrated in real cardiac tissue with drug-induced LQT syndrome (32, 36). This same scenario is also responsible for phase 2 reentry (Supplemental Figure 4), in which the action potential in the central region exhibits a spike-and-dome morphology (Figure 1*b*) whereas the action potential in the surrounding area exhibits early repolarization (short APD) without a dome. Phase 2 reentry initiates reentrant arrhythmias in both acute ischemia and Brugada syndrome (37–39).

3.4.4. Induction of arrhythmias via dynamic instabilities—In the three mechanisms of reentry initiation described above, the heterogeneities can either be preexisting or arise from dynamic instabilities. For example, spatially discordant APD alternans (Figure 4*a*) creates tissue heterogeneity via dynamic instabilities (40, 41), even when all the cells in the tissue have identical properties. Moreover, dynamic instabilities can simultaneously generate triggers and create a heterogeneous substrate that is vulnerable to initiation of reentry by those same triggers. As Sato et al. (14) showed in tissue exhibiting EADs, chaos synchronization results in the formation of tissue islands exhibiting action potentials with EADs next to tissue regions exhibiting action potentials without EADs (Figure 4*b*). If the EADs in these islands have sufficient amplitude to generate triggered activity, the impulses propagate readily into the regions without EADs and may then be blocked when they encounter another island with a long APD, thereby inducing reentry or a mixture of multiple foci and reentry. In the presence of preexisting tissue heterogeneities, dynamic instabilities are generally potentiated, increasing the probability that triggers will induce reentry.

4. ARRHYTHMIA DYNAMICS AT THE CELLULAR SCALE

The tissue-scale wave dynamics are collective behaviors of the myocytes that form the tissue. A single myocyte can exhibit a variety of action potential dynamics, including APD and Ca^{2+} alternans, EADs, DADs, automaticity, and random and chaotic dynamics. Understanding the cellular dynamics is key for understanding the mechanisms of arrhythmias because they are not only important for understanding the tissue-scale mechanisms but also important for mechanistically linking the molecular and subcellular dynamics to the tissue- and organ-scale dynamics.

4.1. Alternans

Pulsus alternans and T-wave alternans are commonly observed clinically and are recognized as precursors of cardiac arrhythmias (42, 43). Because the T-wave is a measure of repolarization in the ventricles, T-wave alternans corresponds to APD alternans at the cellular scale, at which the action potential exhibits a long-short-long-short pattern (Figure 1*f*).

APD alternans can be caused either by instabilities originating from voltage (voltage-driven alternans) or by instabilities originating from Ca^{2+} cycling (Ca^{2+}-driven alternans) (44). However, because voltage and Ca^{2+} are bidirectionally coupled, alternans is always influenced by both factors, although one may predominate over the other, depending on the specific setting.

Voltage-driven alternans can be classified into three categories, all of which are related to APD restitution properties. The first and the most widely studied case is rapid, pacing-induced APD alternans (Figure 1*f*), which is caused by a steep slope of the APD restitution curve at short diastolic intervals. Theoretically, when the slope of the APD restitution curve at the equilibrium state for a given pacing rate exceeds one, the equilibrium state becomes unstable, and the system transitions to a new state. The instability, combined with nonlinear properties of APD restitution, can eventually lead to a stable long-short-long-short alternating pattern (i.e., APD alternans) or to much more complex periodic and frankly chaotic patterns (45, 46). Even though APD restitution is a collective property that arises from the recovery of all ionic currents and their interactions with voltage, the kinetics of recovery of $I_{Ca,L}$ is a particularly key factor regulating the steepness of APD restitution curve at fast heart rates (diastolic interval < 100 ms), because its recovery time constant is typically in this range of the diastolic interval (47). However, all other currents also contribute to the steepness of APD restitution either directly as a result of their own recovery from inactivation kinetics or indirectly by affecting other currents influencing the APD.

A second mechanism of voltage-driven alternans is transient outward K^+ current (I_{to})-driven APD alternans, which occurs at slow or normal heart rates. This type of alternans was first observed in ischemic tissue by Lukas & Antzelevitch (48) and later in a computer model by Hopenfeld (49), who showed that alternans is induced by the sensitive dependence of the spike-and-dome action potential morphology on I_{to}. This mechanism of alternans can be responsible for the T-wave alternans seen in patients with Brugada syndrome (50). The mechanism of this type of alternans is also related to the steepness of APD restitution. However, due to short-term memory effects, the slope of APD restitution curve alone is not an accurate predictor (44). In addition to I_{to}, the slow component of the delayed rectifier K^+ current (I_{Ks}) also plays an important role due to its slow recovery kinetics.

The third mechanism of voltage-driven alternans is APD alternans at normal or slow heart rates caused by the interaction of window and pedestal $I_{Ca,L}$ with I_{Ks}, which can cause the T-wave alternans seen in patients with LQT syndrome (50). Under normal conditions, APD does not change dramatically at slow heart rates, because most of the ion channels are fully recovered. However, under the conditions of reduced repolarization reserve causing EADs, such as in LQT syndrome, APD varies sensitively with heart rate (51), causing alternans and more complex patterns at slow heart rates (52). The two major ionic currents critical to this slow-rate instability are the window and pedestal components of $I_{Ca,L}$ and I_{Ks}. Late I_{Na} [a persistent small conductance due to incomplete inactivation of the Na^+ channel (53–55)] can substitute for or enhance the role of window and pedestal $I_{Ca,L}$.

For Ca^{2+}-driven alternans, two mechanisms have been characterized (56, 57). In the first mechanism, alternans is caused by a steep fractional SR Ca^{2+} release relationship, first

proposed by Eisner et al. (58). Later theoretical analyses (45, 59) showed that, besides a steep fractional SR release relationship, reduced SERCA pump activity is also required. A condition required by this mechanism is that SR Ca^{2+} load alternates concomitantly with cytosolic Ca^{2+}, which was observed in experiments from Eisner's group (60, 61) and others (62). However, later experimental studies also showed that this condition is not met under all circumstances and that cytosolic Ca^{2+} alternans can occur without SR Ca^{2+} load alternans (63, 64). That is, before each beat, the SR loads to the same level, but the amount of Ca^{2+} released exhibits an alternating pattern. These observations supported a different mechanism, in which refractoriness of the Ca^{2+} release channels (RyRs) is the major factor promoting alternans. Under such conditions, SR Ca^{2+} load alternans is not required. Refractoriness alone, however, is not sufficient to induce alternans, unless coupling of the Ca^{2+} release units is also present to allow a Ca^{2+} spark from one Ca^{2+} release unit to recruit a neighboring Ca^{2+} release unit to fire (65–67).

Alternans not only is a precursor but also can be a direct cause of arrhythmias. First, when APD alternans occurs, conduction block can occur at much slower pacing rates due to the long APD on alternate beats (45). Second, in cardiac tissue, APD alternans can be out of phase in different regions, forming spatially discordant APD alternans (Figure 4*a*), resulting in a large dispersion of refractoriness that creates a substrate vulnerable to initiation of reentry (68). Theoretical studies (40, 41) supported by experimental observations (69, 70) show that the formation of spatially discordant alternans requires conduction velocity restitution (Supplemental Figure 2*c*), i.e., a dependence of conduction velocity on its preceding diastolic interval. Because conduction velocity restitution is determined mainly by the recovery of Na^+ channels at very short diastolic intervals, spatially discordant alternans is a cause of arrhythmias only at very fast heart rates in the normal heart (>300 beats per min, as in pacing-induced VF). However, in the presence of Na^+ channel–blocking drugs that slow recovery from inactivation (71), during acute ischemia, or in electrically remodeled diseased hearts, spatially discordant alternans may develop at much slower heart rates (72).

4.2. Early Afterdepolarizations

EADs are voltage oscillations during the plateau and repolarization phases of the action potential (Figure 1*e*) and occur in cardiac diseases such as acquired and congenital LQT syndrome (73, 74) and heart failure (75, 76). In general, EADs occur when outward currents are reduced and/or inward currents are increased (77–80), a condition termed reduced repolarization reserve (81). However, whereas reduced repolarization reserve is sufficient to prolong APD, it is not sufficient to produce EADs. Other conditions are required to generate the voltage oscillations pathognomonic of EADs, which arise from different causes. These conditions are summarized in a recent review article (82) providing a holistic analysis of underlying mechanisms based on nonlinear dynamics. Even though each of the ionic currents in a cardiac myocyte can affect EADs, the most critical to the dynamics of oscillations include window $I_{Ca,L}$, late I_{Na}, and I_{Ks}. In addition, EADs can also be promoted by intracellular Ca^{2+} oscillations (83, 84) or by prolonged Ca^{2+} transients inducing EADs during the rapid repolarization phase of the action potential (phase 3 EADs) via I_{NCX} (85, 86).

A very interesting property of EADs is their sensitive all-or-nothing behavior in response to heart rate changes (Supplemental Figure 5*a*), which result in a steep, nonlinear APD restitution property (Supplemental Figure 5*b*). This nonlinear property can give rise to dynamic chaos (Supplemental Figure 5*c*) (14, 18), which is responsible for the irregularly appearing EAD behavior widely observed in experiments (Supplemental Figure 5*d*). The consequence of the chaotic dynamics at the tissue scale is the induction of dispersion of refractoriness. The dispersion of refractoriness arises from the competition between the chaotic dynamics at the cellular level, which tends to create APD dispersion between cells, and the gap junction coupling at the tissue level, which forces APD to be regionally quasi-uniform. As a result, the chaotic EAD behavior becomes synchronized regionally but desynchronized globally, forming islands of long action potentials with EADs separated by regions without EADs (Figure 4*b*). The presence of preexisting tissue heterogeneity further amplifies this effect. In regions where EADs are too small to propagate, they create dispersion of refractoriness resulting in a tissue substrate vulnerable to reentry; in regions where EADs reach the threshold to propagate (e.g., Figure 3*c*), they generate triggers to initiate reentry. Depending on the cellular and tissue properties, this behavior can result in purely reentrant arrhythmias, multiple shifting foci, and a mixture of multiple shifting foci and reentry (14, 17).

4.3. Delayed Afterdepolarizations

DADs are spontaneous depolarizations during diastole that often occur following a train of rapid pacing (Figure 1*e*) (87). DADs are caused by spontaneous Ca^{2+} release from the SR that propagates as a Ca^{2+} wave through the myocyte (Supplemental Figure 6*a*) (88, 89). During a Ca^{2+} wave, cytoplasmic free Ca^{2+} concentration is elevated, which increases inward I_{NCX} and other Ca^{2+}-sensitive inward currents, causing a depolarization. If the voltage elevation does not reach the threshold for I_{Na} activation, there is only a small voltage deflection. Once the threshold for I_{Na} activation is exceeded, an action potential is elicited (Figure 1*e*). The magnitude of a DAD depends on the magnitude of the Ca^{2+} transient and the conductance of I_{NCX} and I_{K1} (90, 91). DADs are easier to induce in heart failure (91, 92) and CPVT (20, 93–96) than in normal hearts. In both heart failure and CPVT, RyRs become leaky, promoting spontaneous Ca^{2+} waves when the SR becomes Ca^{2+} loaded, e.g., by fast heart rates and adrenergic stimulation. In heart failure, I_{NCX} is upregulated and I_{K1} is downregulated, giving rise to favorable conditions for the formation of superthreshold DADs. The formation of Ca^{2+} waves is a self-organizing critical phenomenon (97, 98), exhibiting large fluctuations and thus resulting in the irregular occurrence of DADs (Supplemental Figure 6*b*). When a DAD triggers an action potential, it can result in a PVC, but when a DAD does not trigger an action potential, it may still create dispersion of excitability, promoting regional conduction block (99). Subthreshold DADs manifest as a U-wave on the electrocardiogram (100, 101). A key issue that still remains to be elucidated is how irregular DADs become synchronized regionally in tissue to induce arrhythmias (102, 103).

4.4. Spike-and-Dome Action Potentials and Early Repolarization

In the ventricles, the higher I_{to} density in epicardial myocytes produces a characteristic spike-and- dome action potential morphology (Figure 1*b*) (104). Even though I_{to} is an

outward current, it can prolong APD via secondary effects on other ion channels (105). If I_{to} is too large, however, the action potential abruptly shortens and loses the spike-and-dome morphology (Supplemental Figure 4*a*,*b*). Due to this steep, nonmonotonic response, alternans and irregular (chaotic) action potential dynamics can occur, as shown in experiments (48) and simulation studies (44, 49, 106, 107). When I_{to} is heterogeneously distributed, the region with the spike-and-dome action potential can propagate during phase 2 into the region with early repolarization and very short APD, inducing phase 2 reentry (Supplemental Figure 4*c*). In computer simulation studies of tissue exhibiting action potential heterogeneity due to I_{to} gradients, phase 2 reentry can be induced over a wide range of parameter space when irregular (chaotic) action potential dynamics are present (106, 107), whereas the parameter space is very narrow otherwise (108). Phase 2 reentry has been demonstrated experimentally (37, 109) and is thought to be a major mechanism of arrhythmias during acute ischemia and in Brugada syndrome (110), although other factors, such as regional fibrosis promoting slow conduction, have also been proposed (111).

4.5. Automaticity

Under normal conditions, ventricular myocytes are excitable cells that remain at rest in the absence of a physiological pacemaker or electrical stimulus. However, ventricular myocytes can become oscillatory under abnormal conditions, termed automaticity (Figure 1*g*), which can generate PVCs or repetitive focal excitations in tissue. Multiple factors can cause automaticity. For example, Na^+ channel inactivation defects, such as aconitine-induced automaticity (112), or I_{K1} reduction (113), cause spontaneous beating. Coupling of myocytes to myofibroblasts via heterocellular gap junctions can also depolarize the myocyte's resting membrane potential sufficiently to induce automaticity (114), which may be relevant to the increased ventricular ectopy seen in diseased hearts with fibrosis. Periodic Ca^{2+} oscillations, similar to the mechanisms causing DAD-mediated triggered activity, can also result in automaticity. The bidirectional coupling of voltage and Ca^{2+} (i.e., voltage affects Ca^{2+} at the same time that Ca^{2+} affects voltage) potentiates this mechanism such that spontaneous Ca^{2+} release elicits an action potential, and consequently, the action potential brings in more Ca^{2+} through Ca^{2+} channels to enhance spontaneous Ca^{2+} release. This coupling process forms a positive feedback loop in a manner similar to that of the Ca^{2+} oscillation that drives the sinoatrial node (115). A third mechanism is similar to that of EADs, in which oscillations mediated by $I_{Ca,L}$ during the plateau become sustained due to failure of full repolarization (30).

4.6. Dynamics Arising from Heterocellular Coupling

The cellular dynamics summarized above do not always arise from myocytes but can emerge from heterocellular coupling of myocytes to nonmyocytes. For example, coupling of a myocyte to a fibroblast/myofibroblast through heterocellular gap junctions can result in automaticity (114), EADs (116), spike-and-dome action potential morphology, and alternans (117). Normal excitable ventricular cells coupled to nonexcitable ischemic ventricular cells may result in sustained oscillations (118). Two cells with different APDs under conditions of reduced repolarization reserve can also result in EADs (36).

5. SUBCELLULAR DYNAMICS AND THE MOLECULAR AND IONIC BASIS OF ARRHYTHMIAS

The cellular dynamics and the corresponding dynamic parameters (e.g., APD, APD restitution, conduction velocity, and conduction velocity restitution) are properties that emerge from the nonlinear interactions between multiple molecular and ionic factors (Figure 5). For example, APD restitution is not controlled by a single current but is a collective behavior of the recovery of all ionic currents and their interactions with voltage. However, some currents have greater influence than others. Moreover, molecular interactions at the subcellular scale, such as Ca^{2+} alternans and Ca^{2+} waves that influence the cellular dynamics through their aggregate effects on ionic currents, create subcellular dynamics. Although complex, the situation is not hopelessly so. Each molecular factor plays a specific role in promoting dynamics that can ultimately be dissected by a combined approach integrating nonlinear dynamics, modeling, and experiment. Here we briefly summarize the roles of some of the key molecular factors promoting the subcellular and cellular dynamics.

5.1. Ion Channels and Transporters

There are many types of ion channels and transporters in the membranes of a ventricular myocyte (Figure 5). Alterations of the ion channel and transporter properties may result in cellular action potential dynamics that lead to arrhythmias at the tissue and organ scales. Here we review their specific roles in generating the cellular action potential dynamics.

5.1.1. Na^+ channels—I_{Na} is the main current responsible for the rapid upstroke of the action potential in ventricular myocytes. By determining the speed of the upstroke (dV/dt_{max}), I_{Na} is a major determinant of excitability and conduction velocity. For this reason, I_{Na} (specifically its recovery from inactivation) largely determines conduction velocity restitution, which is exacerbated in chronic ischemia by slowed recovery from inactivation (119). I_{Na} affects APD indirectly and directly. The amplitude of I_{Na} determines the maximum voltage of the action potential, which affects voltage-dependent activation of other currents influencing action potential repolarization. I_{Na} therefore contributes to APD restitution at very short diastolic intervals when its recovery from inactivation is still incomplete, which in turn affects the stability of reentry. I_{Na} properties also become altered under diseased conditions, failing to inactivate fully during the action potential and thus resulting in late I_{Na}. Late I_{Na} can result from genetic mutations in Na^+ channels, causing LQT3 syndrome, or can be induced by signaling pathways such as Ca^{2+}/calmodulin-dependent protein kinase II (CaMKII) (Figure 5) (53), which is activated in heart failure. Late I_{Na} directly prolongs APD and can cause EADs by reducing repolarization reserve. Moreover, late I_{Na} brings extra Na^+ into the cell, which increases intracellular Na^+ and thus intracellular Ca^{2+} via Na^+-Ca^{2+} exchangers. Elevation of Ca^{2+} can promote Ca^{2+} alternans and waves and further activate the CaMKII signaling pathway, generating more late I_{Na} in a positive feedback loop, with arrhythmogenic consequences (53–55).

5.1.2. L-type Ca^{2+} channels—L-type Ca^{2+} channels play two major roles under normal conditions: triggering Ca^{2+} release from the SR essential for contraction and maintaining the plateau phase of the action potential. Due to the latter, $I_{Ca,L}$ is a major determinant of APD

and thus APD restitution. More importantly, because the time constant of recovery of $I_{Ca,L}$ is less than 100 ms, $I_{Ca,L}$ has a major effect on the steepness of APD restitution at short to intermediate diastolic intervals. Thus, $I_{Ca,L}$ plays an important role in the development of APD alternans at fast heart rates, as well as in spiral wave stability. Blocking $I_{Ca,L}$ suppresses APD alternans and prevents spiral wave breakup (26). The late component of $I_{Ca,L}$ (termed the window and pedestal $I_{Ca,L}$), although relatively small compared with peak $I_{Ca,L}$, plays a key role in promoting EADs (78, 120), as well as APD alternans at slow heart rates (52). In addition, increasing $I_{Ca,L}$ increases Ca^{2+} entry and thus promotes intracellular Ca^{2+} loading, which can promote Ca^{2+} alternans and waves, as well as activating the CaMKII signaling pathway. $I_{Ca,L}$ is regulated by Ca^{2+} in two ways (Figure 5): Ca^{2+} binds with calmodulin to form a Ca^{2+}/calmodulin complex, which causes Ca^{2+}-dependent inactivation to decrease $I_{Ca,L}$, forming a negative feedback loop, and activation of the CaMKII pathway increases $I_{Ca,L}$, forming a positive feedback loop.

5.1.3. K^+ channels—There are a wide variety of K^+ currents in ventricular myocytes (121) (Figure 5), including the fast and slow I_{to} ($I_{to,f}$ and $I_{to,s}$), the fast and slow components of the delayed rectifier K^+ current (I_{Kr} and I_{Ks}), I_{K1}, the plateau K^+ current (I_{Kp}), ATP-sensitive K^+ current [$I_{K(ATP)}$], stretch-activated K^+ current ($I_{SAC,K}$), and small-conductance Ca^{2+}-activated K^+ current (I_{SK}) (122–124). The common role of K^+ currents is to facilitate repolarization of the action potential such that reducing these currents generally lengthens APD. In general, reducing K^+ currents has a larger effect on lengthening APD at slow heart rates than at fast heart rates, resulting in a steeper APD restitution curve, which promotes alternans and spiral wave instability. The reduction in repolarization reserve also promotes EAD-mediated arrhythmias. Due to their different kinetics and Ca^{2+} dependencies, however, different K^+ currents play different roles in promoting these arrhythmogenic dynamics. For example, by enhancing early repolarization reserve, I_{to} lowers the early plateau voltage into the window range of $I_{Ca,L}$ and slows the activation of I_{Ks}, paradoxically reducing late repolarization reserve and promoting EADs (125). In contrast, I_{Ks} activates and deactivates very slowly, thereby preferentially lengthening APD at slow heart rates, which plays a major role in EAD formation. Under conditions of reduced repolarization reserve, slow deactivation of I_{Ks} plays a major role in steepening APD restitution at slow heart rates, which promotes APD alternans at slow heart rates (52). I_{K1} is a time-independent current responsible for phase 3 (rapid repolarization) of the action potential as well as for maintaining a stable diastolic resting potential. Therefore, I_{K1}, like I_{Na}, is a major determinant of both excitability and conduction velocity. For this reason, reduction of I_{K1} is an important contributor to DADs (91), as well as to automaticity (113).

When K^+ currents are enhanced, in contrast, increased repolarization reserve can also promote arrhythmogenic dynamics by different mechanisms. I_{to} produces the spike-and-dome morphology required for phase 2 reentry when repolarization reserve is increased due to either enhanced K^+ conductance or decreased inward conductance, as in Brugada syndrome and short-QT syndrome characterized by gain-of-function mutations in K^+ channels or loss-of-function mutations in Na^+ or Ca^{2+} channels (126). Activation of $I_{K(ATP)}$ serves a similar role in acute ischemia by summing with I_{to} to induce early repolarization promoting phase 2 reentry (37). In addition, mitochondrial depolarization causing $I_{K(ATP)}$

activation during acute ischemia/reperfusion has been proposed to generate regional metabolic sinks that enhance electrical dispersion and create a tissue substrate vulnerable to reentry (127). Recent studies (123, 124) show that I_{SK}, normally expressed in atrial tissue, becomes upregulated in ventricular tissue during heart failure and may promote ventricular arrhythmias by shortening APD relative to the Ca^{2+} transient, promoting EADs in the late part of phase 3 (85, 86, 123, 128).

5.1.4. Ion transporters—Maintaining proper ion gradients across the cell membrane is required for cardiac myocytes to remain excitable and oscillatory. To maintain intracellular ion concentrations, Na^+-Ca^{2+} exchange transports one Ca^{2+} ion for three Na^+ ions, and Na^+-K^+ ATPase transports three Na^+ ions for two K^+ ions. Because both transporters are electrogenic, they affect both action potential and Ca^{2+} cycling dynamics. I_{NCX} prolongs APD and can promote EADs and is also a key player in DADs (91, 129) and automaticity (113). Blocking the Na^+-K^+ pump current (I_{NaK}) causes intracellular Na^+ elevation, which promotes intracellular Ca^{2+} loading via the Na^+-Ca^{2+} exchanger, Ca^{2+} waves, and thus DADs (130).

5.1.5. Miscellaneous ion channels and transporters—Other ion channels and transporters in ventricular myocytes may also play important roles in cellular dynamics. For example, Ca^{2+}-activated nonselective cation channels [$I_{ns(Ca)}$] (14), Ca^{2+}-activated Cl^- channels [$I_{Cl(Ca)}$] (131), and stretch-activated nonselective cation channels [$I_{SAC,ns}$] (132) are inward currents, which may contribute to EAD and DAD formation, as well as influencing repolarization and affecting APD restitution properties. Ion channels and transporters located in intracellular organelles, such as RyRs and SERCA in the SR and a variety of ion channels in mitochondria, also play critical roles in regulating subcellular Ca^{2+} cycling and cardiac energetics. These channels and transporters indirectly affect subcellular and cellular arrhythmia dynamics by modulating the properties of sarcolemmal ion channels and transporters, as discussed in more detail in the next section.

5.2. Ionic Homeostasis and Subcellular Ca^{2+} Cycling Dynamics

Intracellular Ca^{2+} cycling plays multiple critical roles in cardiac arrhythmias (88, 133). First, Ca^{2+} levels during systole and diastole directly affect Ca^{2+}-dependent ionic currents, such as $I_{Ca,L}$, I_{NCX}, I_{Ks}, and I_{SK}, which then modulate cellular action potential dynamics. Second, Ca^{2+} regulates Ca^{2+}-dependent signaling pathways, such as CaMKII, that in turn modulate ionic currents and Ca^{2+} cycling (Figure 5). Third, Ca^{2+} cycling can generate its own arrhythmogenic dynamics, including Ca^{2+} alternans and Ca^{2+} waves. As shown by recent studies, these dynamics are self-organizing phenomena of spatiotemporal systems. A ventricular myocyte contains more than 20,000 Ca^{2+} release units, which are coupled by Ca^{2+} diffusion via Ca^{2+}-induced Ca^{2+} release. Each Ca^{2+} release unit contains a RyR cluster in which the RyRs fire collectively, producing an all-or-nothing, localized Ca^{2+} release event termed a Ca^{2+} spark (134, 135). Ca^{2+} sparks are random events but also have their own complex dynamics (135–137). Ca^{2+} alternans is a self-organized phenomenon arising from the interaction of Ca^{2+} sparks (i.e., the coupling of Ca^{2+} release units), as analyzed in our recent theoretical studies (56, 65, 66). In addition, different patterns of spatiotemporal subcellular Ca^{2+} alternans dynamics, including spatially discordant alternans (138) and

transition from microscopic alternans to macroscopic alternans (139), have been demonstrated. The transition from Ca^{2+} sparks to Ca^{2+} waves reflects a signaling hierarchy: individual sparks, spark clusters, abortive waves, and persistent waves (140, 141), which can be described by the theory of criticality (97, 98). Three general properties of a diffusively coupled Ca^{2+} release unit network can account for the essential dynamics: random activation, refractoriness, and recruitment [the 3R theory (56)]. Self-organized criticality can be used to explain why Ca^{2+} waves occur much later than RyR recovery and SR refilling time, a time delay termed the idle period (142). In the formation of both Ca^{2+} alternans and Ca^{2+} waves, the coupling of Ca^{2+} release units plays a key role.

Dysregulation of intracellular Na^+ can also promote arrhythmogenic dynamics (143). Elevation of intracellular Na^+ enhances the Na^+-K^+ pump (increasing outward I_{NaK}) but slows intracellular Ca^{2+} removal by Na^+-Ca^{2+} exchange (decreasing inward I_{NCX}). These effects tend to shorten the action potential and elevate intracellular Ca^{2+}, which can promote arrhythmogenic Ca^{2+} cycling dynamics. The presence of late I_{Na} can cause Na^+ overload, which then causes Ca^{2+} overload, facilitating CaMKII activation. CaMKII activation in turn amplifies late I_{Na} in a positive feedback loop, potentiating arrhythmia dynamics (53–55).

K^+ (particularly extracellular K^+) also affects arrhythmia dynamics. Normal extracellular [K^+] concentration is 3.5 to 5 mM, and both lower and higher extracellular [K^+] can cause arrhythmias. Specifically, elevation of extracellular [K^+] depolarizes resting membrane potential and increases I_{K1} and I_{Kr}, which shortens the action potential. Elevation of the resting potential first increases and then slows conduction velocity, eventually resulting in conduction failure. In contrast, lowering extracellular [K^+] decreases I_{K1} and I_{Kr}, which lengthens APD and destabilizes the resting potential. Lengthening APD can promote EADs, as well as increased Ca^{2+} loading. Lowering extracellular [K^+] also inhibits the Na^+-K^+ pump, further promoting Na^+ and Ca^{2+} overload. Ca^{2+} overload can then activate the CaMKII signaling pathway, which further potentiates Na^+ and Ca^{2+} loading by increasing late I_{Na} and $I_{Ca,L}$. These effects act synergistically to promote arrhythmogenic cellular action potential dynamics, such as alternans, EADs, and DADs.

5.3. Genetic Factors

Genetic mutations in ion channels, transporters, and their regulatory and trafficking partners that predispose to cardiac arrhythmias have provided powerful insights illuminating the molecular basis of cardiac arrhythmias (4, 5). Although too broad a field to review in detail here, channelopathies that are caused by gene mutations, such as LQT syndrome, CPVT, short-QT syndrome, and Brugada syndrome, have been highly informative. So far, 13 genes for LQT, 4 genes for CVPT, and 7 genes for Brugada syndrome, with hundreds of mutations, have been identified (126, 144). A mutation may cause gain or loss of function that affects action potential or Ca^{2+} cycling dynamics through the dynamic mechanisms outlined above. For example, LQT mutations lengthen APD and predispose the myocytes to EADs, whereas CPVT mutations increase the RyR open probability and predispose the myocytes to DADs. A single gene mutation may have multiple consequences for cellular dynamics and disease phenotypes. For example, Na^+ channel mutation 1795insD can cause both LQT syndrome and Brugada syndrome (145). Although genetic channelopathies are

relatively rare, they share important commonalities with ventricular arrhythmias associated with common diseases. For example, arrhythmias in the setting of heart failure recapitulate features of LQT syndromes (e.g., reduced repolarization reserve promoting EAD-mediated arrhythmias such as polymorphic VT), and arrhythmias during acute ischemia recapitulate features of Brugada syndrome (phase 2 reentry). Both types of arrhythmias recapitulate features of CPVT (abnormal Ca^{2+} cycling promoting alternans, Ca^{2+} waves, and DAD-mediated arrhythmias).

5.4. Signaling Pathways

By modifying ion channel and transporter properties at the molecular level, a variety of signaling pathways critically influence arrhythmia dynamics (133, 146, 147–149), both acutely through post-translational modification of their protein targets (e.g., phosphorylation) and chronically by altering transcription, trafficking, and protein turnover (electrical remodeling, including gap junction remodeling). In addition to their effects on sarcolemmal ion channels/transporters, these signaling pathways also regulate Ca^{2+} cycling elements both acutely and chronically (excitation-contraction coupling remodeling), as well as gap junction coupling (gap junction remodeling). These pathways alter cellular metabolism (metabolic remodeling) and influence (*a*) nonmyocytes such as fibroblasts (structural remodeling), (*b*) vascular components (vascular remodeling), and (*c*) neural components (neural remodeling). Although too broad a field to review here, the most widely studied signaling pathways include the adrenergic/cholinergic, angiotensin/aldosterone, and CaMKII/calcineurin axes. They promote arrhythmias through their effects on Ca^{2+} cycling and ionic currents, as well as through modifying tissue coupling properties. Figure 5 plots part of the signaling pathways of protein kinases A and C and CaMKII and their effects on the SERCA pump, RyRs, and many ionic currents. By destabilizing subcellular-, cellular-, and tissue-scale dynamics and exacerbating tissue heterogeneity, these signaling pathways play a key role in increasing the susceptibility of the heart to arrhythmias.

6. CONCLUDING REMARKS

As this article reviews, cardiac dynamics are regulated by multiple factors operating over different temporal and spatial scales in a complex interactive network. We can briefly summarize the important general concepts as follows. First, molecular-scale events, such as genetic mutations, signaling, and metabolism, regulate ion channel and Ca^{2+} cycling properties. Second, the ionic currents determine the action potential and intracellular ion concentrations, but they are also regulated by voltage and ion concentrations as well as by signaling pathways. Third, Ca^{2+} cycling can independently give rise to arrhythmogenic subcellular and cellular dynamics. Fourth, because Ca^{2+} and voltage are bidirectionally coupled, the feedback loops between them give rise to a rich variety of cellular action potential dynamics. Fifth, the cellular action potential dynamics combined with tissue-scale factors promote tissue-scale dynamics, creating tissue substrates that generate focal excitations and are susceptible to initiation of reentry due to electrical dispersion. Sixth, the systems dynamics at the organism scale activate reflexes that feed back to the molecular level through activation of a variety of signaling pathways. Finally, even though these multiscale interactions are very complex, the two key hubs are voltage and Ca^{2+}.

Understanding the action potential and Ca^{2+} cycling dynamics is critical for relating molecular-scale events to the development of ventricular arrhythmias.

Table 1 summarizes our current understanding of the subcellular, cellular, and tissue-scale action potential and Ca^{2+} cycling dynamics, their corresponding mechanisms, their electrocardiographic characteristics, and their link to clinical diseases. We hope that this can be a useful platform that will facilitate the quest to move beyond engineering approaches (devices and ablation) to treat ventricular arrhythmias and to move toward the development of novel biological approaches. In this quest, we note that, even in the normal heart, lethal arrhythmias can be induced by rapid pacing or electrical shocks. In other words, from a dynamics perspective, both sinus rhythm and arrhythmias are solutions of the normal heart as well as the diseased heart. The occurrence of arrhythmias is a probabilistic transition from sinus rhythm to turbulent ventricular behavior. In the view of nonlinear dynamics, the objective of an effective therapy is to elevate the threshold governing the transition from sinus rhythm to arrhythmias without markedly altering normal sinus rhythm, i.e., to enlarge the basin of attraction of normal sinus rhythm while suppressing the basin of attraction of arrhythmias.

To achieve this goal, however, there are considerable challenges to overcome. First, a given molecular target, such as an ion channel, often has effects on multiple aspects of arrhythmia dynamics such that a drug effective at treating one mechanism may worsen another, potentially substituting one lethal arrhythmia for another. For example, class I antiarrhythmic drugs, which block Na^+ channels, can successfully suppress PVCs. The CAST trial (6) was designed to test the hypothesis that suppressing PVCs with class I antiarrhythmic drugs would reduce mortality by reducing arrhythmia triggers. However, such drugs also lower excitability, especially in ischemic hearts, enhancing the vulnerability of the tissue substrate to reentry, which led to a higher death rate in the treated group in the CAST trial (6). Class III antiarrhythmic drugs, which block K^+ channels, lengthen APD to prevent reentry. The SWORD trial (7) was designed to test the hypothesis that lengthening APD with class III antiarrhythmic drugs would reduce mortality by preventing reentry. However, these drugs also reduce repolarization reserve and promote EADs, which may have caused increased mortality in the treated group in the SWORD trial (7). Therefore, the ideal therapeutic intervention should suppress all dynamic mechanisms of arrhythmias described above or, at the very least, suppress one without exacerbating the others. Second, the occurrence of arrhythmias, especially VF, is unpredictable. These events are rare events, even when potential triggering events such as PVCs are common. One of the greatest challenges is to predict which patients are at the highest risk and need to be treated, whether by biologics or device therapy. In our view, future efforts not only should focus on specific arrhythmia mechanisms but also should require a systems view of ventricular arrhythmias to accurately predict arrhythmia risk, to identify the right therapeutic targets, and to develop effective and robust therapeutics.

Supplementary Material

Refer to Web version on PubMed Central for supplementary material.

LITERATURE CITED

1. Janse MJ, Rosen MR. History of arrhythmias. Handb Exp Pharmacol. 2006; 2006:1–39. [PubMed: 16610339]
2. Jalife J. Ventricular fibrillation: mechanisms of initiation and maintenance. Annu Rev Physiol. 2000; 62:25–50. [PubMed: 10845083]
3. Zipes DP, Wellens HJ. Sudden cardiac death. Circulation. 1998; 98:2334–51. [PubMed: 9826323]
4. Priori SG, Napolitano C. Genetics of cardiac arrhythmias and sudden cardiac death. Ann N Y Acad Sci. 2004; 1015:96–110. [PubMed: 15201152]
5. Marsman RF, Tan HL, Bezzina CR. Genetics of sudden cardiac death caused by ventricular arrhythmias. Nat Rev Cardiol. 2014; 11:96–111. [PubMed: 24322550]
6. CAST I. Effect of encainide and flecainide on mortality in a random trial of arrhythmia suppression after myocardial infarction. N Engl J Med. 1989; 321:406–12. [PubMed: 2473403]
7. Waldo AL, Camm AJ, deRuyter H, Friedman PL, Macneil DJ, et al. Effect of d-sotalol on mortality in patients with left ventricular dysfunction after recent and remote myocardial infarction. Lancet. 1996; 348:7–12. [PubMed: 8691967]
8. Myerburg RJ, Mitrani R, Interian A, Castellanos A. Interpretation of outcomes of antiarrhythmic clinical trials: design features and population impact. Circulation. 1998; 97:1514–21. [PubMed: 9576433]
9. Tung R, Zimetbaum P, Josephson ME. A critical appraisal of implantable cardioverter-defibrillator therapy for the prevention of sudden cardiac death. J Am Coll Cardiol. 2008; 52:1111–21. [PubMed: 18804736]
10. Qu Z, Hu G, Garfinkel A, Weiss JN. Nonlinear and stochastic dynamics in the heart. Phys Rep. 2014; 543:61–162. [PubMed: 25267872]
11. O'Reilly CM, Fogarty KE, Drummond RM, Tuft RA, Walsh JV. Quantitative analysis of spontaneous mitochondrial depolarizations. Biophys J. 2003; 85:3350–57. [PubMed: 14581236]
12. Aon MA, Cortassa S, Marban E, O'Rourke B. Synchronized whole cell oscillations in mitochondrial metabolism triggered by a local release of reactive oxygen species in cardiac myocytes. J Biol Chem. 2003; 278:44735–44. [PubMed: 12930841]
13. Xie Y, Sato D, Garfinkel A, Qu Z, Weiss JN. So little source, so much sink: requirements for afterdepolarizations to propagate in tissue. Biophys J. 2010; 99:1408–15. [PubMed: 20816052]
14. Sato D, Xie LH, Sovari AA, Tran DX, Morita N, et al. Synchronization of chaotic early afterdepolarizations in the genesis of cardiac arrhythmias. PNAS. 2009; 106:2983–88. [PubMed: 19218447]
15. Asano Y, Davidenko JM, Baxter WT, Gray RA, Jalife J. Optical mapping of drug-induced polymorphic arrhythmias and torsade de pointes in the isolated rabbit heart. J Am Coll Cardiol. 1997; 29:831–42. [PubMed: 9091531]
16. Choi B-R, Burton F, Salama G. Cytosolic Ca^{2+} triggers early afterdepolarizations and torsade de pointes in rabbit hearts with type 2 long QT syndrome. J Physiol. 2002; 543:615–31. [PubMed: 12205194]
17. de Lange E, Xie Y, Qu Z. Synchronization of early afterdepolarizations and arrhythmogenesis in heterogeneous cardiac tissue models. Biophys J. 2012; 103:365–73. [PubMed: 22853915]
18. Sato D, Xie LH, Nguyen TP, Weiss JN, Qu Z. Irregularly appearing early afterdepolarizations in cardiac myocytes: random fluctuations or dynamical chaos? Biophys J. 2010; 99:765–73. [PubMed: 20682253]
19. Qu Z. Chaos in the genesis and maintenance of cardiac arrhythmias. Prog Biophys Mol Biol. 2011; 105:247–57. [PubMed: 21078337]
20. Cerrone M, Noujaim SF, Tolkacheva EG, Talkachou A, O'Connell R, et al. Arrhythmogenic mechanisms in a mouse model of catecholaminergic polymorphic ventricular tachycardia. Circ Res. 2007; 101:1039–48. [PubMed: 17872467]
21. Baher AA, Uy M, Xie F, Garfinkel A, Qu Z, Weiss JN. Bidirectional ventricular tachycardia: ping pong in the His–Purkinje system. Heart Rhythm. 2011; 8:599–605. [PubMed: 21118730]

22. Mines GR. On circulating excitation on heart muscles and their possible relation to tachycardia and fibrillation. Trans R Soc Can. 1914; 4:43–52.
23. Winfree AT. Spiral waves of chemical activity. Science. 1972; 175:634–36. [PubMed: 17808803]
24. Davidenko JM, Pertsov AM, Salomonsz R, Baxter W, Jalife J. Stationary and drifting spiral waves of excitation in isolated cardiac muscle. Nature. 1992; 355:349–51. [PubMed: 1731248]
25. Qu Z, Xie F, Garfinkel A, Weiss JN. Origins of spiral wave meander and breakup in a two-dimensional cardiac tissue model. Ann Biomed Eng. 2000; 28:755–71. [PubMed: 11016413]
26. Wu TJ, Lin SF, Weiss JN, Ting CT, Chen PS. Two types of ventricular fibrillation in isolated rabbit hearts—importance of excitability and action potential duration restitution. Circulation. 2002; 106:1859–66. [PubMed: 12356642]
27. Moe GK, Rheinboldt WC, Abildskov JA. A computer model of atrial fibrillation. Am Heart J. 1964; 67:200–20. [PubMed: 14118488]
28. Chang MG, Sato D, de Lange E, Lee J-H, Karagueuzian HS, et al. Bi-stable wave propagation and early afterdepolarization–mediated cardiac arrhythmias. Heart Rhythm. 2012; 9:115–22. [PubMed: 21855520]
29. Chang MG, de Lange E, Calmettes G, Garfinkel A, Qu Z, Weiss JN. Pro- and antiarrhythmic effects of ATP-sensitive potassium current activation on reentry during early afterdepolarization–mediated arrhythmias. Heart Rhythm. 2013; 10:575–82. [PubMed: 23246594]
30. Vandersickel N, Kazbanov IV, Nuitermans A, Weise LD, Pandit R, Panfilov AV. A study of early afterdepolarizations in a model for human ventricular tissue. PLOS ONE. 2014; 9:e84595. [PubMed: 24427289]
31. Gadsby DC, Cranefield PF. Two levels of resting potential in cardiac Purkinje fibers. J Gen Physiol. 1977; 70:725–46. [PubMed: 591921]
32. Yan G-X, Wu Y, Liu T, Wang J, Marinchak RA, Kowey PR. Phase 2 early afterdepolarization as a trigger of polymorphic ventricular tachycardia in acquired long-QT syndrome: direct evidence from intracellular recordings in the intact left ventricular wall. Circulation. 2001; 103:2851–56. [PubMed: 11401944]
33. Nguyen TP, Qu Z, Weiss JN. Cardiac fibrosis and arrhythmogenesis: The road to repair is paved with perils. J Mol Cell Cardiol. 2014; 70C:83–91. [PubMed: 24184999]
34. Rohr S, Kucera JP, Fast VG, Kleber AG. Paradoxical improvement of impulse conduction in cardiac tissue by partial cellular uncoupling. Science. 1997; 275:841–44. [PubMed: 9012353]
35. Janse MJ, Wit AL. Electrophysiological mechanisms of ventricular arrhythmias resulting from myocardial ischemia and infarction. Physiol Rev. 1989; 69:1046–169.
36. Maruyama M, Lin SF, Xie Y, Chua SK, Joung B, et al. Genesis of phase 3 early afterdepolarizations and triggered activity in acquired long-QT syndrome. Circ Arrhythm Electrophysiol. 2011; 4:103–11. [PubMed: 21078812]
37. Lukas A, Antzelevitch C. Phase 2 reentry as a mechanism of initiation of circus movement reentry in canine epicardium exposed to simulated ischemia. Cardiovasc Res. 1996; 32:593–603. [PubMed: 8881520]
38. Yan GX, Antzelevitch C. Cellular basis for the Brugada syndrome and other mechanisms of arrhythmogenesis associated with ST-segment elevation. Circulation. 1999; 100:1660–66. [PubMed: 10517739]
39. Yan GX, Joshi A, Guo D, Hlaing T, Martin J, et al. Phase 2 reentry as a trigger to initiate ventricular fibrillation during early acute myocardial ischemia. Circulation. 2004; 110:1036–41. [PubMed: 15302777]
40. Echebarria B, Karma A. Instability and spatiotemporal dynamics of alternans in paced cardiac tissue. Phys Rev Lett. 2002; 88:208101. [PubMed: 12005608]
41. Qu Z, Garfinkel A, Chen PS, Weiss JN. Mechanisms of discordant alternans and induction of reentry in simulated cardiac tissue. Circulation. 2000; 102:1664–70. [PubMed: 11015345]
42. Rosenbaum DS, Jackson LE, Smith JM, Garan H, Ruskin JN, Cohen RJ. Electrical alternans and vulnerability to ventricular arrhythmias. N Engl J Med. 1994; 330:235–41. [PubMed: 8272084]
43. Verrier RL, Klingenheben T, Malik M, El-Sherif N, Exner DV, et al. Microvolt T-wave alternans physiological basis, methods of measurement, and clinical utility—consensus guideline by

International Society for Holter and Noninvasive Electrocardiology. J Am Coll Cardiol. 2011; 58:1309–24. [PubMed: 21920259]

44. Qu Z, Xie Y, Garfinkel A, Weiss JN. T-wave alternans and arrhythmogenesis in cardiac diseases. Front Physiol. 2010; 1:154. [PubMed: 21286254]
45. Qu Z, Shiferaw Y, Weiss JN. Nonlinear dynamics of cardiac excitation-contraction coupling: an iterated map study. Phys Rev E. 2007; 75:011927.
46. Chialvo DR, Gilmour RF, Jalife J. Low dimensional chaos in cardiac tissue. Nature. 1990; 343:653–57. [PubMed: 2304537]
47. Mahajan A, Shiferaw Y, Sato D, Baher A, Olcese R, et al. A rabbit ventricular action potential model replicating cardiac dynamics at rapid heart rates. Biophys J. 2008; 94:392–410. [PubMed: 18160660]
48. Lukas A, Antzelevitch C. Differences in the electrophysiological response of canine ventricular epicardium and endocardium to ischemia. Role of the transient outward current. Circulation. 1993; 88:2903–15. [PubMed: 8252704]
49. Hopenfeld B. Mechanism for action potential alternans: the interplay between L-type calcium current and transient outward current. Heart Rhythm. 2006; 3:345–52. [PubMed: 16500310]
50. Wegener FT, Ehrlich JR, Hohnloser SH. Amiodarone-associated macroscopic T-wave alternans and torsade de pointes unmasking the inherited long QT syndrome. Europace. 2008; 10:112–13. [PubMed: 18006559]
51. Antzelevitch C. Heterogeneity of cellular repolarization in LQTS: the role of M cells. Eur Heart J Suppl. 2001; 3:K2–16.
52. Qu Z, Chung D. Mechanisms and determinants of ultralong action potential duration and slow rate-dependence in cardiac myocytes. PLOS ONE. 2012; 7:e43587. [PubMed: 22952713]
53. Wagner S, Ruff HM, Weber SL, Bellmann S, Sowa T, et al. Reactive oxygen species–activated Ca/calmodulin kinase IIδ is required for late I_{Na} augmentation leading to cellular Na and Ca overload. Circ Res. 2011; 108:555–65. [PubMed: 21252154]
54. Wasserstrom JA, Sharma R, O'Toole MJ, Zheng J, Kelly JE, et al. Ranolazine antagonizes the effects of increased late sodium current on intracellular calcium cycling in rat isolated intact heart. J Pharmacol Exp Ther. 2009; 331:382–91. [PubMed: 19675298]
55. Song Y, Shryock JC, Belardinelli L. An increase of late sodium current induces delayed afterdepolarizations and sustained triggered activity in atrial myocytes. Am J Physiol Heart Circ Physiol. 2008; 294:H2031–39. [PubMed: 18310511]
56. Qu Z, Nivala M, Weiss JN. Calcium alternans in cardiac myocytes: order from disorder. J Mol Cell Cardiol. 2013; 58:100–9. [PubMed: 23104004]
57. Escobar AL, Valdivia HH. Cardiac alternans and ventricular fibrillation: a bad case of ryanodine receptors reneging on their duty. Circ Res. 2014; 114:1369–71. [PubMed: 24763460]
58. Eisner DA, Choi HS, Diaz ME, O'Neill SC, Trafford AW. Integrative analysis of calcium cycling in cardiac muscle. Circ Res. 2000; 87:1087–94. [PubMed: 11110764]
59. Shiferaw Y, Watanabe MA, Garfinkel A, Weiss JN, Karma A. Model of intracellular calcium cycling in ventricular myocytes. Biophys J. 2003; 85:3666–86. [PubMed: 14645059]
60. Diaz ME, O'Neill SC, Eisner DA. Sarcoplasmic reticulum calcium content fluctuation is the key to cardiac alternans. Circ Res. 2004; 94:650–56. [PubMed: 14752033]
61. Li Y, Diaz ME, Eisner DA, O'Neill S. The effects of membrane potential, SR Ca^{2+} content and RyR responsiveness on systolic Ca^{2+} alternans in rat ventricular myocytes. J Physiol. 2009; 587:1283–92. [PubMed: 19153161]
62. Xie LH, Sato D, Garfinkel A, Qu Z, Weiss JN. Intracellular Ca alternans: coordinated regulation by sarcoplasmic reticulum release, uptake, and leak. Biophys J. 2008; 95:3100–10. [PubMed: 18539635]
63. Picht E, DeSantiago J, Blatter LA, Bers DM. Cardiac alternans do not rely on diastolic sarcoplasmic reticulum calcium content fluctuations. Circ Res. 2006; 99:740–48. [PubMed: 16946134]
64. Shkryl VM, Maxwell JT, Domeier TL, Blatter LA. Refractoriness of sarcoplasmic reticulum Ca release determines Ca alternans in atrial myocytes. Am J Physiol Heart Circ Physiol. 2012; 302:H2310–20. [PubMed: 22467301]

65. Rovetti R, Cui X, Garfinkel A, Weiss JN, Qu Z. Spark-induced sparks as a mechanism of intracellular calcium alternans in cardiac myocytes. Circ Res. 2010; 106:1582–91. [PubMed: 20378857]
66. Nivala M, Qu Z. Calcium alternans in a couplon network model of ventricular myocytes: role of sarcoplasmic reticulum load. Am J Physiol Heart Circ Physiol. 2012; 303:H341–52. [PubMed: 22661509]
67. Restrepo JG, Weiss JN, Karma A. Calsequestrin-mediated mechanism for cellular calcium transient alternans. Biophys J. 2008; 95:3767–89. [PubMed: 18676655]
68. Pastore JM, Girouard SD, Laurita KR, Akar FG, Rosenbaum DS. Mechanism linking T-wave alternans to the genesis of cardiac fibrillation. Circulation. 1999; 99:1385–94. [PubMed: 10077525]
69. Hayashi H, Shiferaw Y, Sato D, Nihei M, Lin SF, et al. Dynamic origin of spatially discordant alternans in cardiac tissue. Biophys J. 2007; 92:448–60. [PubMed: 17071663]
70. Mironov S, Jalife J, Tolkacheva EG. Role of conduction velocity restitution and short-term memory in the development of action potential duration alternans in isolated rabbit hearts. Circulation. 2008; 118:17–25. [PubMed: 18559701]
71. Pu JL, Balser JR, Boyden PA. Lidocaine action on Na^+ currents in ventricular myocytes from the epicardial border zone of the infarcted heart. Circ Res. 1998; 83:431–40. [PubMed: 9721700]
72. Qu Z, Karagueuzian HS, Garfinkel A, Weiss JN. Effects of Na^+ channel and cell coupling abnormalities on vulnerability to reentry: a simulation study. Am J Physiol Heart Circ Physiol. 2004; 286:H1310–21. [PubMed: 14630634]
73. Keating MT, Sanguinetti MC. Molecular and cellular mechanisms of cardiac arrhythmias. Cell. 2001; 104:569–80. [PubMed: 11239413]
74. Liu GX, Choi B-R, Ziv O, Li W, de Lange E, et al. Differential conditions for early afterdepolarizations and triggered activity in cardiomyocytes derived from transgenic LQT1 and LQT2 rabbits. J Physiol. 2012; 590:1171–80. [PubMed: 22183728]
75. Nuss HB, Kaab S, Kass DA, Tomaselli GF, Marban E. Cellular basis of ventricular arrhythmias and abnormal automaticity in heart failure. Am J Physiol Heart Circ Physiol. 1999; 277:H80–91.
76. Li GR, Lau CP, Ducharme A, Tardif JC, Nattel S. Transmural action potential and ionic current remodeling in ventricles of failing canine hearts. Am J Physiol Heart Circ Physiol. 2002; 283:H1031–41. [PubMed: 12181133]
77. Damiano BP, Rosen MR. Effects of pacing on triggered activity induced by early afterdepolarizations. Circulation. 1984; 69:1013–25. [PubMed: 6705157]
78. January CT, Riddle JM. Early afterdepolarizations: mechanism of induction and block. A role for L-type Ca^{2+} current. Circ Res. 1989; 64:977–90. [PubMed: 2468430]
79. January CT, Moscucci A. Cellular mechanisms of early afterdepolarizations. Ann N Y Acad Sci. 1992; 644:23–32. [PubMed: 1562117]
80. Zeng J, Rudy Y. Early afterdepolarizations in cardiac myocytes: mechanism and rate dependence. Biophys J. 1995; 68:949–64. [PubMed: 7538806]
81. Roden DM. Taking the “idio” out of “idiosyncratic”: predicting torsades de pointes. Pacing Clin Electrophysiol. 1998; 21:1029–34. [PubMed: 9604234]
82. Qu Z, Xie L-H, Olcese R, Karagueuzian HS, Chen P-S, et al. Early afterdepolarizations in cardiac myocytes: beyond reduced repolarization reserve. Cardiovasc Res. 2013; 99:6–15. [PubMed: 23619423]
83. Volders PG, Vos MA, Szabo B, Sipido KR, de Groot SH, et al. Progress in the understanding of cardiac early afterdepolarizations and torsades de pointes: time to revise current concepts. Cardiovasc Res. 2000; 46:376–92. [PubMed: 10912449]
84. Zhao Z, Wen H, Fefelova N, Allen C, Baba A, et al. Revisiting the ionic mechanisms of early afterdepolarizations in cardiomyocytes: predominant by Ca waves or Ca currents? Am J Physiol Heart Circ Physiol. 2012; 302:H1636–44. [PubMed: 22307670]
85. Burashnikov A, Antzelevitch C. Reinduction of atrial fibrillation immediately after termination of the arrhythmia is mediated by late phase 3 early afterdepolarization–induced triggered activity. Circulation. 2003; 107:2355–60. [PubMed: 12695296]

86. Maruyama M, Ai T, Chua S-K, Park H-W, Lee Y-S, et al. Hypokalemia promotes late phase 3 early afterdepolarization and recurrent ventricular fibrillation during isoproterenol infusion in Langendorff perfused rabbit ventricles. Heart Rhythm. 2014; 11:697–706. [PubMed: 24378768]
87. Yeh YH, Wakili R, Qi XY, Chartier D, Boknik P, et al. Calcium-handling abnormalities underlying atrial arrhythmogenesis and contractile dysfunction in dogs with congestive heart failure. Circ Arrhythm Electrophysiol. 2008; 1:93–102. [PubMed: 19808399]
88. ter Keurs HEDJ, Boyden PA. Calcium and arrhythmogenesis. Physiol Rev. 2007; 87:457–506. [PubMed: 17429038]
89. Xie L-H, Chen F, Karagueuzian HS, Weiss JN. Oxidative stress–induced afterdepolarizations and calmodulin kinase II signaling. Circ Res. 2009; 104:79–86. [PubMed: 19038865]
90. Maruyama M, Joung B, Tang L, Shinohara T, On YK, et al. Diastolic intracellular calcium-membrane voltage coupling gain and postshock arrhythmias: role of Purkinje fibers and triggered activity. Circ Res. 2010; 106:399–408. [PubMed: 19926871]
91. Pogwizd SM, Schlotthauer K, Li L, Yuan W, Bers DM. Arrhythmogenesis and contractile dysfunction in heart failure: roles of sodium-calcium exchange, inward rectifier potassium current, and residual β-adrenergic responsiveness. Circ Res. 2001; 88:1159–67. [PubMed: 11397782]
92. Pogwizd SM, Bers DM. Calcium cycling in heart failure: the arrhythmia connection. J Cardiovasc Electrophysiol. 2002; 13:88–91. [PubMed: 11843491]
93. Hilliard FA, Steele DS, Laver D, Yang Z, Le Marchand SJ, et al. Flecainide inhibits arrhythmogenic Ca^{2+} waves by open state block of ryanodine receptor Ca^{2+} release channels and reduction of Ca^{2+} spark mass. J Mol Cell Cardiol. 2010; 48:293–301. [PubMed: 19835880]
94. Lehnart SE, Mongillo M, Bellinger A, Lindegger N, Chen BX, et al. Leaky Ca^{2+} release channel/ryanodine receptor 2 causes seizures and sudden cardiac death in mice. J Clin Investig. 2008; 118:2230–45. [PubMed: 18483626]
95. Jiang D, Xiao B, Yang D, Wang R, Choi P, et al. RyR2 mutations linked to ventricular tachycardia and sudden death reduce the threshold for store-overload-induced Ca^{2+} release (SOICR). PNAS. 2004; 101:13062–67. [PubMed: 15322274]
96. Dirksen WP, Lacombe VA, Chi M, Kalyanasundaram A, Viatchenko-Karpinski S, et al. A mutation in calsequestrin, CASQ2D307H, impairs sarcoplasmic reticulum Ca^{2+} handling and causes complex ventricular arrhythmias in mice. Cardiovasc Res. 2007; 75:69–78. [PubMed: 17449018]
97. Nivala M, Ko CY, Nivala M, Weiss JN, Qu Z. Criticality in intracellular calcium signaling in cardiac myocytes. Biophys J. 2012; 102:2433–42. [PubMed: 22713558]
98. Nivala M, Ko CY, Nivala M, Weiss JN, Qu Z. The emergence of subcellular pacemaker sites for calcium waves and oscillations. J Physiol. 2013; 591:5305–20. [PubMed: 24042497]
99. Rosen MR, Wit AL, Hoffman BF. Electrophysiology and pharmacology of cardiac arrhythmias. IV. Cardiac antiarrhythmic and toxic effects of digitalis. Am Heart J. 1975; 89:391–99. [PubMed: 1090138]
100. Surawicz B. U wave: facts, hypotheses, misconceptions, and misnomers. J Cardiovasc Electrophysiol. 1998; 9:1117–28. [PubMed: 9817564]
101. di Bernardo D, Murray A. Origin on the electrocardiogram of U-waves and abnormal U-wave inversion. Cardiovasc Res. 2002; 53:202–8. [PubMed: 11744029]
102. Fujiwara K, Tanaka H, Mani H, Nakagami T, Takamatsu T. Burst emergence of intracellular Ca^{2+} waves evokes arrhythmogenic oscillatory depolarization via the Na^{+}-Ca^{2+} exchanger: simultaneous confocal recording of membrane potential and intracellular Ca^{2+} in the heart. Circ Res. 2008; 103:509–18. [PubMed: 18635824]
103. Wasserstrom JA, Shiferaw Y, Chen W, Ramakrishna S, Patel H, et al. Variability in timing of spontaneous calcium release in the intact rat heart is determined by the time course of sarcoplasmic reticulum calcium load. Circ Res. 2010; 107:1117–26. [PubMed: 20829511]
104. Di Diego JM, Sun ZQ, Antzelevitch C. I(to) and action potential notch are smaller in left versus right canine ventricular epicardium. Am J Physiol Heart Circ Physiol. 1996; 271:H548–61.
105. Greenstein JL, Wu R, Po S, Tomaselli GF, Winslow RL. Role of the calcium-independent transient outward current I_{to1} in shaping action potential morphology and duration. Circ Res. 2000; 87:1026–33. [PubMed: 11090548]

106. Maoz A, Krogh-Madsen T, Christini DJ. Instability in action potential morphology underlies phase 2 reentry: a mathematical modeling study. Heart Rhythm. 2009; 6:813–22. [PubMed: 19467510]
107. Cantalapiedra IR, Penaranda A, Mont L, Brugada J, Echebarria B. Reexcitation mechanisms in epicardial tissue: role of I_{to} density heterogeneities and I_{Na} inactivation kinetics. J Theor Biol. 2009; 259:850–59. [PubMed: 19410581]
108. Miyoshi S, Mitamura H, Fujikura K, Fukuda Y, Tanimoto K, et al. A mathematical model of phase 2 reentry: role of L-type Ca current. Am J Physiol Heart Circ Physiol. 2003; 284:H1285–94. [PubMed: 12531737]
109. Di Diego JM, Antzelevitch C. High $[Ca^{2+}]_o$-induced electrical heterogeneity and extrasystolic activity in isolated canine ventricular epicardium. Phase 2 reentry. Circulation. 1994; 89:1839–50. [PubMed: 7511994]
110. Antzelevitch C. Ion channels and ventricular arrhythmias: cellular and ionic mechanisms underlying the Brugada syndrome. Curr Opin Cardiol. 1999; 14:274–79. [PubMed: 10358800]
111. Coronel R, Casini S, Koopmann TT, Wilms-Schopman FJG, Verkerk AO, et al. Right ventricular fibrosis and conduction delay in a patient with clinical signs of Brugada syndrome: a combined electrophysiological, genetic, histopathologic, and computational study. Circulation. 2005; 112:2769–77. [PubMed: 16267250]
112. Scherf D. Studies on auricular tachycardia caused by aconitine administration. Proc Soc Exp Biol Med. 1947; 64:839–44.
113. Silva J, Rudy Y. Mechanism of pacemaking in I_{K1}-downregulated myocytes. Circ Res. 2003; 92:261–63. [PubMed: 12595336]
114. Miragoli M, Salvarani N, Rohr S. Myofibroblasts induce ectopic activity in cardiac tissue. Circ Res. 2007; 101:755–58. [PubMed: 17872460]
115. Lakatta EG, Maltsev VA, Vinogradova TM. A coupled system of intracellular Ca^{2+} clocks and surface membrane voltage clocks controls the timekeeping mechanism of the heart's pacemaker. Circ Res. 2010; 106:659–73. [PubMed: 20203315]
116. Nguyen TP, Xie Y, Garfinkel A, Qu Z, Weiss JN. Arrhythmogenic consequences of myofibroblast-myocyte coupling. Cardiovasc Res. 2012; 93:242–51. [PubMed: 22049532]
117. Xie Y, Garfinkel A, Weiss JN, Qu Z. Cardiac alternans induced by fibroblast-myocyte coupling: mechanistic insights from computational models. Am J Physiol Heart Circ Physiol. 2009; 297:H775–84. [PubMed: 19482965]
118. Keener JP. Model for the onset of fibrillation following coronary artery occlusion. J Cardiovasc Electrophysiol. 2003; 14:1225–32. [PubMed: 14678140]
119. Pinto JM, Boyden PA. Electrical remodeling in ischemia and infarction. Cardiovasc Res. 1999; 42:284–97. [PubMed: 10533567]
120. Madhvani RV, Xie Y, Pantazis A, Garfinkel A, Qu Z, et al. Shaping a new Ca^{2+} conductance to suppress early afterdepolarizations in cardiac myocytes. J Physiol. 2011; 589:6081–92. [PubMed: 22025660]
121. Nerbonne JM. Molecular basis of functional voltage-gated K^+ channel diversity in the mammalian myocardium. J Physiol. 2000; 525(Part 2):285–98. [PubMed: 10835033]
122. Tuteja D, Xu D, Timofeyev V, Lu L, Sharma D, et al. Differential expression of small-conductance Ca^{2+}-activated K^+ channels SK1, SK2, and SK3 in mouse atrial and ventricular myocytes. Am J Physiol Heart Circ Physiol. 2005; 289:H2714–23. [PubMed: 16055520]
123. Chua SK, Chang PC, Maruyama M, Turker I, Shinohara T, et al. Small-conductance calcium-activated potassium channel and recurrent ventricular fibrillation in failing rabbit ventricles. Circ Res. 2011; 108:971–79. [PubMed: 21350217]
124. Chang P-C, Hsieh Y-C, Hsueh C-H, Weiss JN, Lin S-F, Chen P-S. Apamin induces early afterdepolarizations and torsades de pointes ventricular arrhythmia from failing rabbit ventricles exhibiting secondary rises in intracellular calcium. Heart Rhythm. 2013; 10:1516–24. [PubMed: 23835258]
125. Zhao Z, Xie Y, Wen H, Xiao D, Allen C, et al. Role of the transient outward potassium current in the genesis of early afterdepolarizations in cardiac cells. Cardiovasc Res. 2012; 95:308–16. [PubMed: 22660482]

126. Kaufman ES. Mechanisms and clinical management of inherited channelopathies: long QT syndrome, Brugada syndrome, catecholaminergic polymorphic ventricular tachycardia, and short QT syndrome. Heart Rhythm. 2009; 6:S51–55. [PubMed: 19631908]

127. Akar FG, Aon MA, Tomaselli GF, O'Rourke B. The mitochondrial origin of postischemic arrhythmias. J Clin Investig. 2005; 115:3527–35. [PubMed: 16284648]

128. Tang L, Joung B, Ogawa M, Chen P-S, Lin S-F. Intracellular calcium dynamics, shortened action potential duration, and late-phase 3 early afterdepolarization in Langendorff-perfused rabbit ventricles. J Cardiovasc Electrophysiol. 2012; 23:1364–71. [PubMed: 22809087]

129. Sugai Y, Miura M, Hirose M, Wakayama Y, Endoh H, et al. Contribution of Na^+/Ca^{2+} exchange current to the formation of delayed afterdepolarizations in intact rat ventricular muscle. J Cardiovasc Pharmacol. 2009; 53:517–22. [PubMed: 19487959]

130. Rosen, M.; Danilo, P, Jr. Digitalis-induced delayed afterdepolarizations. In: Zipes, D.; Bailey, J.; Elharrar, V., editors. The Slow Inward Current and Cardiac Arrhythmias. Dordrecht, Neth: Springer; 1980. p. 417-35.

131. Verkerk AO, Tan HL, Kirkels JH, Ravesloot JH. Role of Ca^{2+}-activated Cl^- current during proarrhythmic early afterdepolarizations in sheep and human ventricular myocytes. Acta Physiol Scand. 2003; 179:143–48. [PubMed: 14510777]

132. Reed A, Kohl P, Peyronnet R. Molecular candidates for cardiac stretch-activated ion channels. Glob Cardiol Sci Pract. 2014; 2014:19.

133. Bers DM. Calcium cycling and signaling in cardiac myocytes. Annu Rev Physiol. 2008; 70:23–49. [PubMed: 17988210]

134. Cheng H, Lederer WJ. Calcium sparks. Physiol Rev. 2008; 88:1491–545. [PubMed: 18923188]

135. Stern MD, Rios E, Maltsev VA. Life and death of a cardiac calcium spark. J Gen Physiol. 2013; 142:257–74. [PubMed: 23980195]

136. Sobie EA, Song LS, Lederer WJ. Restitution of Ca^{2+} release and vulnerability to arrhythmias. J Cardiovasc Electrophysiol. 2006; 17(Suppl 1):64–70.

137. Winslow RL, Greenstein JL. Extinguishing the sparks. Biophys J. 2013; 104:2115–17. [PubMed: 23708349]

138. Gaeta SA, Bub G, Abbott GW, Christini DJ. Dynamical mechanism for subcellular alternans in cardiac myocytes. Circ Res. 2009; 105:335–42. [PubMed: 19628792]

139. Tian Q, Kaestner L, Lipp P. Noise-free visualization of microscopic calcium signaling by pixel-wise fitting. Circ Res. 2012; 111:17–27. [PubMed: 22619280]

140. Cheng H, Lederer MR, Lederer WJ, Cannell MB. Calcium sparks and $[Ca^{2+}]_i$ waves in cardiac myocytes. Am J Physiol Cell Physiol. 1996; 270:C148–59.

141. Wier WG, ter Keurs HE, Marban E, Gao WD, Balke CW. Ca^{2+} "sparks" and waves in intact ventricular muscle resolved by confocal imaging. Circ Res. 1997; 81:462–69. [PubMed: 9314826]

142. Belevych AE, Terentyev D, Terentyeva R, Ho HT, Gyorke I, et al. Shortened Ca^{2+} signaling refractoriness underlies cellular arrhythmogenesis in a postinfarction model of sudden cardiac death. Circ Res. 2012; 110:569–77. [PubMed: 22223353]

143. O'Rourke B, Maack C. The role of Na dysregulation in cardiac disease and how it impacts electrophysiology. Drug Discov Today Dis Models. 2007; 4:207–17. [PubMed: 18650959]

144. Webster G, Berul CI. An update on channelopathies: from mechanisms to management. Circulation. 2013; 127:126–40. [PubMed: 23283857]

145. Clancy CE, Rudy Y. Na^+ channel mutation that causes both Brugada and long-QT syndrome phenotypes: a simulation study of mechanism. Circulation. 2002; 105:1208–13. [PubMed: 11889015]

146. Wagner S, Rokita AG, Anderson ME, Maier LS. Redox regulation of sodium and calcium handling. Antioxid Redox Signal. 2013; 18:1063–77. [PubMed: 22900788]

147. Dobrev D, Wehrens XHT. Role of RyR2 phosphorylation in heart failure and arrhythmias: controversies around ryanodine receptor phosphorylation in cardiac disease. Circ Res. 2014; 114:1311–19. [PubMed: 24723656]

148. Jeong E-M, Liu M, Sturdy M, Gao G, Varghese ST, et al. Metabolic stress, reactive oxygen species, and arrhythmia. J Mol Cell Cardiol. 2012; 52:454–63. [PubMed: 21978629]

149. Swaminathan PD, Purohit A, Hund TJ, Anderson ME. Calmodulin-dependent protein kinase II: linking heart failure and arrhythmias. Circ Res. 2012; 110:1661–77. [PubMed: 22679140]

150. Boyden PA, Dun W, Barbhaiya C, Ter Keurs HE. 2APB- and JTV519(K201)-sensitive micro Ca^{2+} waves in arrhythmogenic Purkinje cells that survive in infarcted canine heart. Heart Rhythm. 2004; 1:218–26. [PubMed: 15851156]

151. Lipp P, Niggli E. Microscopic spiral waves reveal positive feedback in subcellular calcium signaling. Biophys J. 1993; 65:2272–76. [PubMed: 8312468]

152. Xie F, Qu Z, Yang J, Baher A, Weiss JN, Garfinkel A. A simulation study of the effects of cardiac anatomy in ventricular fibrillation. J Clin Investig. 2004; 113:686–93. [PubMed: 14991066]

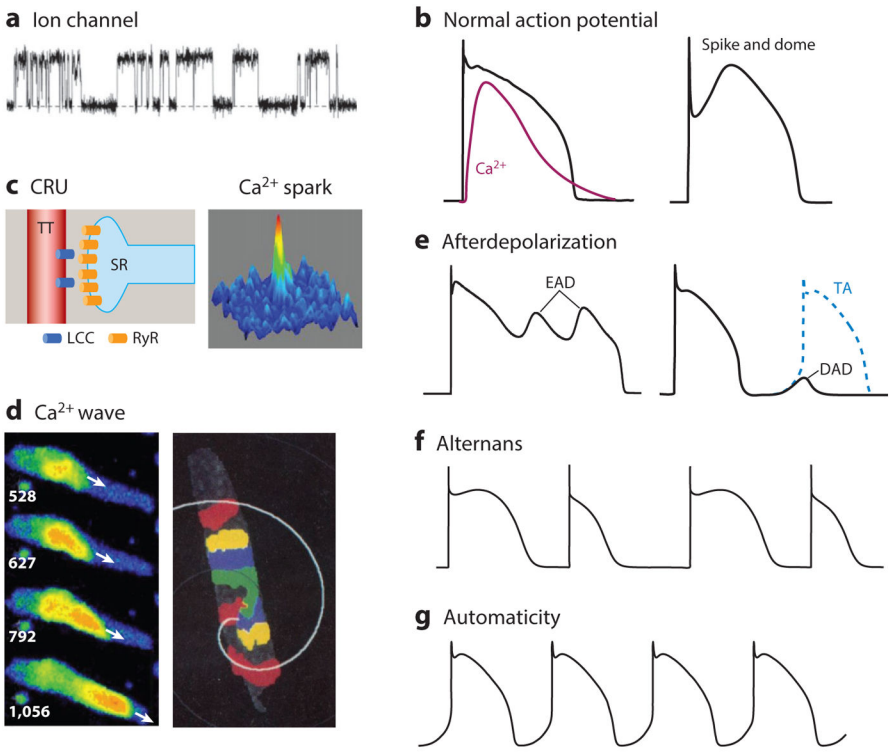

Figure 1.

Subcellular and cellular dynamics of ventricular myocytes. (*a*) A single ion channel opening and closing stochastically. (*b*) Normal action potentials and Ca^{2+} transient for endocardial myocytes (*left*) and epicardial myocytes (*right*). A spike-and-dome morphology occurs in epicardial myocytes. (*c*) A Ca^{2+} release unit (CRU) that is composed of a ryanodine receptor (RyR) cluster in the sarcoplasmic reticulum (SR) membrane and an L-type Ca^{2+} channel (LCC) cluster in the apposing T-tubule (TT) membrane (*left*) and a Ca^{2+} spark (*right*). The spark image was downloaded from https://sites.google.com/site/sparkmasterhome/faq. (*d*) A planar Ca^{2+} wave (*left; arrows* indicate the direction of propagation, and the *numbers* indicate time in milliseconds) from a Purkinje cell (from Reference 150 with permission) and a spiral Ca^{2+} wave (*right*) (from Reference 151 with permission). (*e*) Early afterdepolarizations (EADs), delayed afterdepolarizations (DADs), and triggered activity (TA). (*f*) Action potential alternans. (*g*) Spontaneous oscillations (automaticity).

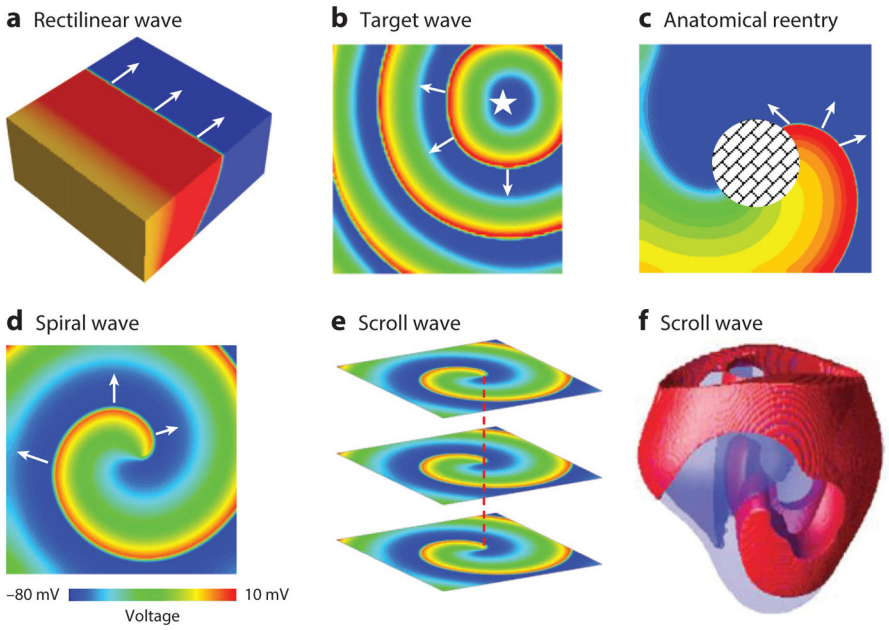

Figure 2.

Tissue-scale excitation dynamics. (*a*) A rectilinear (planar) wave. (*b*) A focal excitation (target wave). (*c*) Reentry around an obstacle. (*d*) A spiral wave. (*e*) A scroll wave. (*f*) A scroll wave in the ventricles (from Reference 152 with permission). Voltage levels are indicated by the color bar, and arrows indicate the directions of propagation in panels *a–e*. In panel *f*, only voltage higher than a certain value is colored in red for three-dimensional visualization.

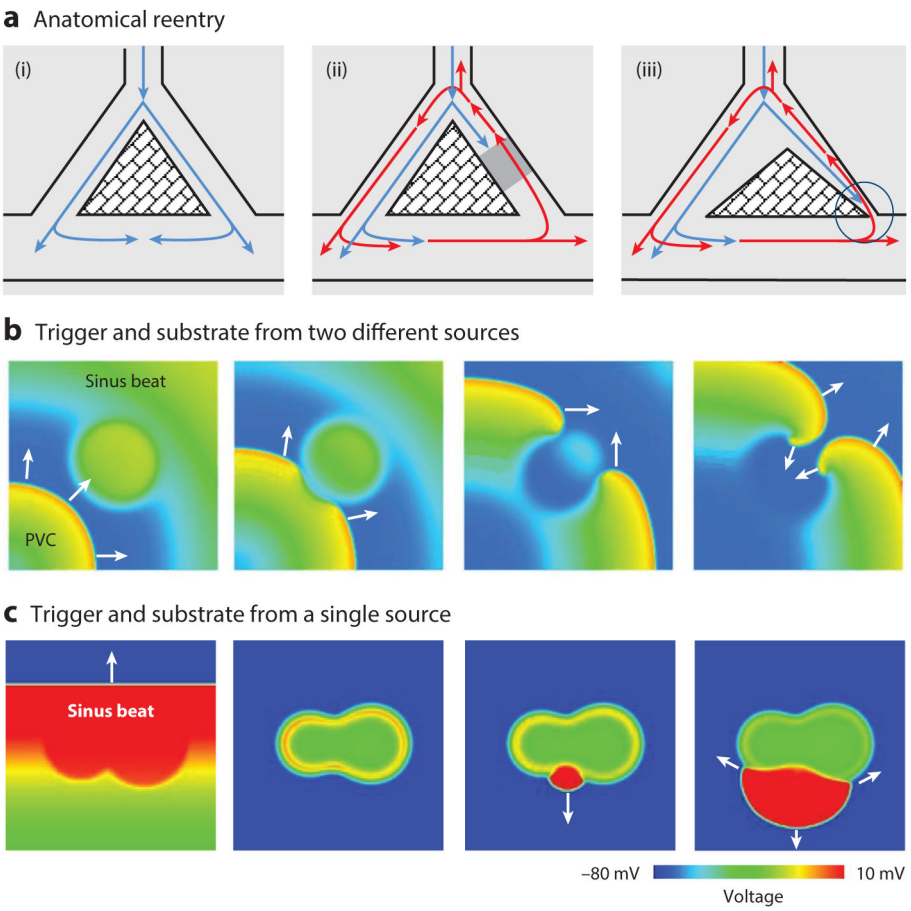

Figure 3.

Mechanisms of reentry initiation. (*a*) Reentry around an anatomic obstacle. (*i*) Homogeneous refractoriness: A premature ventricular complex (PVC) successfully propagates through both sides of the obstacle without forming reentry. (*ii*) Heterogeneous refractoriness: The refractory period in one region is longer than elsewhere (e.g., the *gray zone* in the *right pathway*) such that a properly timed PVC is blocked in the right pathway, propagates successfully through the contralateral pathway (e.g., the *left*), and then reenters the right pathway from the retrograde direction, initiating reentry around the obstacle (*red arrows*). (*iii*) Narrow pathway: The right pathway has a very narrow exit (indicated by the *circle*) such that a PVC cannot conduct out of the pathway, but the impulse from outside can enter the pathway, resulting in reentry (*red arrows*). (*b*) Reentry in heterogeneous tissue in which the central region has a longer refractory period than the rest of the tissue. (*c*) Reentry induction by a trigger and substrate from the same source. Cells in the central region exhibit early afterdepolarizations.

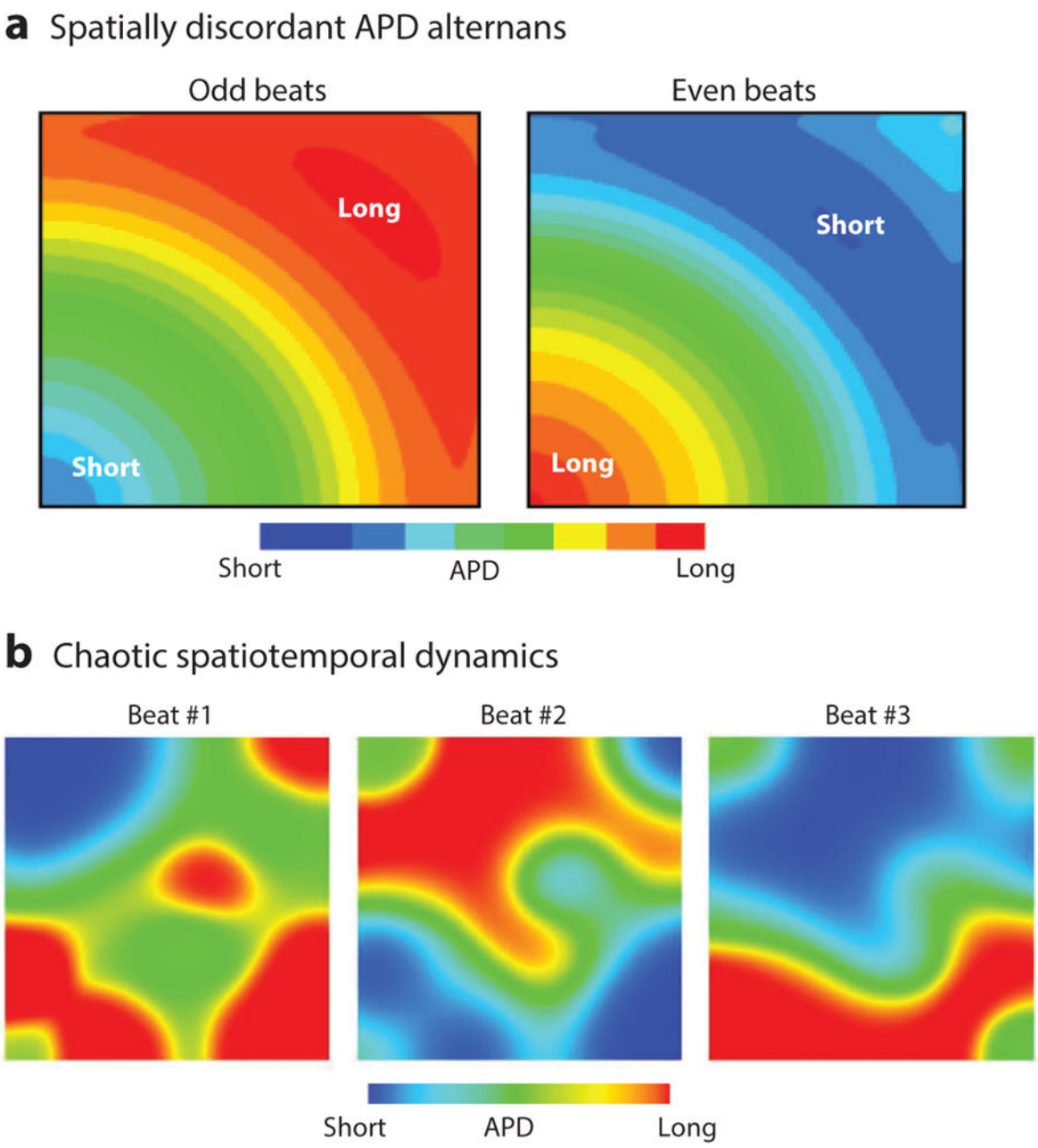

Figure 4.

Dynamically induced dispersion of refractoriness. (*a*) Spatially discordant action potential duration (APD) alternans in which APD is short in one region but long in another region. In the following beat, the spatial APD pattern is reversed. (*b*) Spatiotemporal chaotic dynamics in the presence of early afterdepolarizations (EADs). The APD distribution in tissue exhibits an irregular spatial pattern and varies from beat to beat. EADs occur in long-APD regions (*red*), but not in short-APD regions (*blue*).

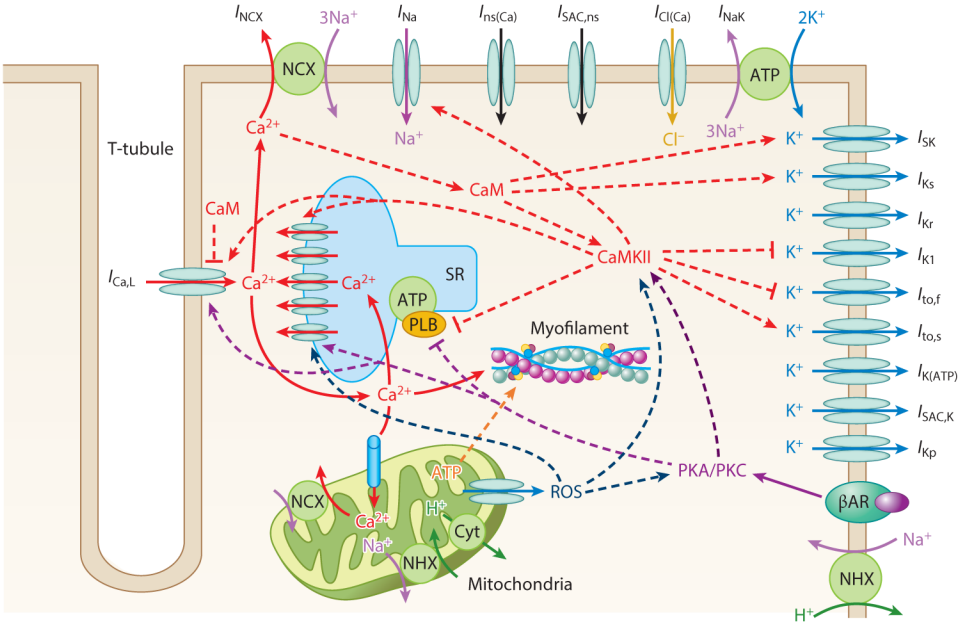

Figure 5.

Schematic diagram of ionic currents, transporters, signaling pathways, and their interactions in a ventricular myocyte. A dashed line with arrow indicates that signaling enhances activity, and a dashed line with bar indicates suppression of activity. See text for details.

Table 1

From subcellular/cellular/tissue dynamics to arrhythmias

Cellular (subcellular) dynamics	Tissue dynamics	Dynamic mechanisms/parameters	ECG characteristics	Related disease conditions
APD and Ca^{2+} alternans, chaos	APD and Ca^{2+} alternans, DOR, reentry	Steep APDR and CVR, steep FSRCR, 3R theory	TWA	LQTS, BS, HF, ischemia
EAD (Ca^{2+} oscillations)	Foci, DOR, biexcitability	RRR, Hopf bifurcation, steep APDR, chaos synchronization	PVC, TWA, NSVT, TdP	LQTS, HF
DAD (Ca^{2+} wave)	Foci	Criticality, synchronization	PVC, U-wave	CPVT, HF
Spike-and-dome	Phase 2 reentry	ERR, APDR, chaos	TWA, J-wave	BS, ERS, SQTS, acute ischemia
Automaticity (Ca^{2+} oscillations)	Foci	Hopf bifurcation, synchronization	PVC, NSVT	Idioventricular rhythms

Abbreviations: 3R theory, theory of Ca^{2+} alternans involving random activation, refractoriness, and recruitment of Ca^{2+} release units; APD, action potential duration; APDR, APD restitution; BS, Brugada syndrome; CPVT, catecholaminergic polymorphic ventricular tachycardia; CVR, conduction velocity restitution; DAD, delayed afterdepolarization; DOR, dispersion of refractoriness; EAD, early afterdepolarization; ECG, electrocardiogram; ERR, enhanced repolarization reserve; ERS, early repolarization syndrome; FSRCR, fractional sarcoplasmic reticulum Ca^{2+} release; HF, heart failure; LQTS, long-QT syndrome; NSVT, nonsustained ventricular tachycardia; PVC, premature ventricular complex; RRR, reduced repolarization reserve; SQTS, short-QT syndrome; TdP, torsade de pointes; TWA, T-wave alternans.